Stability analysis of a new type of inverse Lax-Wendroff boundary treatment of central difference schemes for parabolic equations

Tingting Li[1], and Yan Jiang[2] [3]

Abstract: In this paper, we construct a new type of simplified inverse Lax-Wendroff procedure (SILW) of high order central finite difference schemes for the diffusion equation with initial-boundary value conditions by improving the method in [15]. Comparing with the work in [15], an extra auxiliary parameter is added, providing a more general and flexible method. Stability analysis is also performed for the new type of SILW method. The third order total variation diminishing (TVD) Runge-Kutta method is taken as our time-stepping method in the fully-discrete case. The Godunov-Ryabenkii theory and the eigenvalue spectrum visualization method are adopted to investigate stability for both semi-discrete and fully-discrete cases, a detailed analysis reveals that this two techniques yield similar results. Theoretically, the new proposed SILW method has an improvement in stability, especially for higher order schemes. Numerical tests are provided to validate the stability analysis results.

Key Words: high order central difference schemes; parabolic equation; a new type of simplified inverse Lax-Wendroff procedure; Godunov-Ryabenkii theory; eigenvalue analysis

1 Introduction

There exists many methods in the field of numerical solutions of partial differential equations (PDEs), such as, finite difference method, finite element method, spectral method, collocation method, etc. Of the many difference approaches to solving PDEs numerically, the finite difference method has the advantages of simplicity, directness and high computational efficiency, which is widely used in engineering applications. The high order central difference scheme can achieve high order accuracy with smaller stencil, but it still cannot be utilized near the boundary points directly for initial-boundary value problems (IBVPs), thus we need to construct proper numerical boundary conditions. As stated in [28], there are two issues should be addressed appropriately in the construction

[1]School of Mathematics and Statistics, Henan University, Kaifeng, Henan 475000, China. E-mail: ltt901120@henu.edu.cn. Research is supported by NSFC grant 11801143, 12371393 and Natural Science Foundation of Henan 242300421047.

[2]School of Mathematical Sciences, University of Science and Technology of China, Hefei, Anhui 230026, P.R. China. E-mail: jiangy@ustc.edu.cn. Research is supported by NSFC grant 12271499.

[3]Laoshan Laboratory, Qingdao 266237, China.

of numerical boundary conditions for finite difference methods. Firstly, the evaluation of the ghost point values located outside the computational domain which are used by the interior schemes. Secondly, if the grid points do not coincide with the physical boundary exactly, especially when a Cartesian mesh is used to solve problems on a complex geometry or moving boundary problems, then the so-called "cut-cell" problem arises, which leads to a restricted time step for the sake of stability [2]. The body-fitted meshes [1, 8] method could accurately satisfy boundary conditions at the boundary, but in the case of moving boundary domain, it will result in heavy calculations to get the meshes on each time step. With a non-boundary fitted mesh which is simple and has low complexity, there are many carefully designed methods for the numerical boundary treatments for IBVPs, such as the embedded boundary method [10, 23], the inverse Lax-Wendroff method (ILW) [28] and the simplified inverse Lax-Wendroff method (SILW) [4, 11, 12, 13, 14, 17, 18, 29, 30, 32] and so on. The SILW method uses Taylor expansion at the boundary point to get the approximation values on the ghost points. Derivatives at the boundary points are obtained by the ILW procedure or the interpolation polynomial based on the interior point values, see [12, 13, 14] for details. Thus, the boundary treatment is appropriate for finite difference methods on Cartesian meshes. Moreover, the SILW method has the following advantages: one is the numerical boundary conditions can achieve arbitrary high order accuracy to further maintain the high accuracy globally, and the other one is, it can avoid the cut-cell problem and keep stability under the maximum CFL condition of the scheme for the corresponding Cauchy problem, i.e., the boundary treatment does not effect the stability of the interior schemes. However, for higher order schemes, more terms with the ILW procedure are required, leading to complicated calculation. In [16], the author developed a new type of SILW method for hyperbolic equations, the new type of SILW method substitutes "interpolation" and "extrapolation" for Taylor expansion to get the values of ghost points, and theoretical analysis indicates that comparing with the original SILW method, especially for higher order accuracy, the new proposed one would require fewer terms using the relatively complicated ILW procedure and thus improve computational efficiency on the premise of maintaining accuracy and stability. In [15], the new type of SILW method is extended to solve parabolic and convection-diffusion equations with fourth order central difference method. In this paper, we will propose a new type of SILW method by improving the method in [15] and focus on the stability for high order central finite difference schemes when solving diffusion problems.

General stability analysis for IBVPs on a bounded domain can be performed by the normal mode analysis, which is based on the Laplace transform. This method was firstly

presented by Godunov and Ryabenkii [5] and then developed by Kreiss [9] and Osher [19]. The original Godunov-Ryabenkii theory only provided a necessary condition for stability. In [7], Gustafsson, Kreiss and Sundström proposed the *GKS theory*, which is a necessary and sufficient condition for stability for linear, first order hyperbolic systems in one space dimension. Some other related work can be found in [21, 24, 25]. Stability analysis for parabolic problems was formulated in [20, 26, 31]. And stability analysis for semi-discrete case was studied in [27]. Theoretically, the Godunov-Ryabenkii method leads to necessary conditions for stability, but in a vast number of cases they also appear to be sufficient conditions [26]. The drawback of the Godunov-Ryabenkii method is that it will lead to high algebraic complexity for high order schemes. In [32], the eigenvalue spectrum visualization method was proposed to analyze stability by visualizing the eigenvalues spectrum of the discretization operators and they obtained consistent stability conclusions with the Godunov-Ryabenkii analysis. In our previous work [11, 12, 13, 14], both the the Godunov-Ryabenkii method and eigenvalue analysis were used to analyze stability for hyperbolic and parabolic equations and the two methods produced consistent stability conclusions.

In this paper, we are interested in constructing high order difference schemes for parabolic equations with Dirichlet or Neumann boundary conditions. The high order central difference is taken as our interior scheme, and a new type of SILW method is performed near the boundaries. Following the idea in [15], the new one also utilizes "interpolation" and "extrapolation" to get the values of ghost points, that we impose values of some artificial auxiliary points through a polynomial interpolating the interior points near the boundary, and then construct a Hermite extrapolation based on those auxiliary point values and the spatial derivatives at boundary obtained via the ILW procedure. This polynomial will give us the approximation to the ghost point value. However, different form the method in [15], a more general and flexible method is designed to get the artificial auxiliary points and the method in [15] is a special issue of our method in this paper. Both Godunov-Ryabenkii analysis and eigenvalue spectrum visualization method are used to perform stability analysis, revealing that the new type of SILW method has better performance, which will be shown in detail later.

This paper is organized as follows. In Sect. 2, we review the high order central difference schemes as the interior schemes and the third order total variation diminishing (TVD) Runge-Kutta time discretization method used to get the fully-discrete schemes. The new type SILW method is introduced in detail in this section as well. In Sect. 3, stability analysis is performed both for the semi-discrete and fully-discrete cases by the Godunov-Ryabenkii method and the eigenvalue spectrum visualization method. In Sect.

4, numerical examples are given to demonstrate and validate the results of the analysis. Concluding remarks are given in Sect. 5.

2 Scheme formulation

In this section, firstly, we will introduce the high order central difference schemes which are used as the interior schemes in this paper. Secondly, the third order explicit total variation diminishing (TVD) Runge-Kutta time discretization method [22] are introduced as the time discretization method. Lastly, we will give a detailed description of the new type of SILW method for the boundary treatments.

2.1 High order central difference schemes

Consider the one-dimensional linear scalar heat equation

$$\begin{cases} u_t = c\, u_{xx}, & x \in (a,b), \quad t > 0, \\ u(x,0) = u_0(x), & x \in (a,b), \end{cases} \tag{2.1}$$

with appropriate boundary conditions. For instance, we can take Dirichlet boundary conditions as

$$\begin{cases} u(a,t) = g_1(t), \\ u(b,t) = g_2(t), \end{cases} \quad t \geq 0, \tag{2.2}$$

or Neumann boundary conditions as

$$\begin{cases} u_x(a,t) = g_3(t), \\ u_x(b,t) = g_4(t), \end{cases} \quad t \geq 0. \tag{2.3}$$

Here $c > 0$ is restricted by the well-posedness of the IBVP (2.1).

The interval (a,b) is discretized by a uniform mesh as

$$a + C_a \Delta x = x_0 < x_1 < x_2 < \cdots < x_N = b - C_b \Delta x \tag{2.4}$$

with the uniform mesh size $\Delta x = (b-a)/(C_a+C_b+N)$, and the parameters $C_a, C_b \in [0,1)$. $\{x_j = a + (C_a + j)\,\Delta x,\ j = 0,1,2,\cdots N\}$ are the inner grid points. Note that the first and last points x_0 and x_N are not necessarily aligned with the boundaries, and we choose this kind of discretization on purpose.

In this paper, we consider the second, fourth, sixth, eighth and tenth order central difference schemes. The corresponding semi-discrete schemes are listed below.

- Second order scheme

$$\frac{du_j}{dt} = \frac{c}{\Delta x^2}\,(u_{j+1} - 2u_j + u_{j-1}).$$

- Fourth order scheme

$$\frac{du_j}{dt} = \frac{c}{\Delta x^2}\,(-\frac{1}{12}u_{j-2} + \frac{4}{3}u_{j-1} - \frac{5}{2}u_j + \frac{4}{3}u_{j+1} - \frac{1}{12}u_{j+2}).$$

- Sixth order scheme

$$\frac{du_j}{dt} = \frac{c}{\Delta x^2}\,(\frac{1}{90}u_{j-3} - \frac{3}{20}u_{j-2} + \frac{3}{2}u_{j-1} - \frac{49}{18}u_j + \frac{3}{2}u_{j+1} - \frac{3}{20}u_{j+2} + \frac{1}{90}u_{j+3}).$$

- Eighth order scheme

$$\begin{aligned}\frac{du_j}{dt} = \frac{c}{\Delta x^2}\,(&-\frac{1}{560}u_{j-4} + \frac{8}{315}u_{j-3} - \frac{1}{5}u_{j-2} + \frac{8}{5}u_{j-1} - \frac{205}{72}u_j \\ &+ \frac{8}{5}u_{j+1} - \frac{1}{5}u_{j+2} + \frac{8}{315}u_{j+3} - \frac{1}{560}u_{j+4}).\end{aligned}$$

- Tenth order scheme

$$\begin{aligned}\frac{du_j}{dt} = \frac{c}{\Delta x^2}\,(&\frac{1}{3150}u_{j-5} - \frac{5}{1008}u_{j-4} + \frac{5}{126}u_{j-3} - \frac{5}{21}u_{j-2} + \frac{5}{3}u_{j-1} - \frac{5269}{1800}u_j \\ &+ \frac{5}{3}u_{j+1} - \frac{5}{21}u_{j+2} + \frac{5}{126}u_{j+3} - \frac{5}{1008}u_{j+4} + \frac{1}{3150}u_{j+5}).\end{aligned}$$

In these formulas, u_j is the numerical approximation of the exact solution u at the grid point x_j. Then the semi-discrete interior scheme can be written as

$$U_t = \mathcal{L}(U)\,, \tag{2.5}$$

where $\mathcal{L}$ is spatial discrete operator.

2.2 Time discretization

We take the third order explicit total variation diminishing (TVD) Runge-Kutta (RK) method [22] as our time-stepping method to solve the semi-discrete scheme (2.5) which is a system of ordinary differential equations. We briefly introduce it below for clarity.

From the time level t_n to $t_{n+1} = t_n + \Delta t$, the third order TVD-RK method is given by

$$\begin{aligned}u^{(1)} &= u^n + \Delta t\mathcal{L}(u^n),\\ u^{(2)} &= \frac{3}{4}u^n + \frac{1}{4}u^{(1)} + \frac{1}{4}\Delta t\mathcal{L}(u^{(1)}),\\ u^{n+1} &= \frac{1}{3}u^n + \frac{2}{3}u^{(2)} + \frac{2}{3}\Delta t\mathcal{L}(u^{(2)}).\end{aligned} \tag{2.6}$$

Other types of time discretizations can also be analyzed along the same line.

To avoid order reduction, special attention must be paid when we impose time-dependent boundary conditions in the two intermediate stages of the Runge-Kutta method [3]. With the given Dirichlet boundary condition $g(t)$, the corresponding boundary conditions are given as follows,

$$\begin{aligned} u^n &\sim g(t_n), \\ u^{(1)} &\sim g(t_n) + \Delta t g'(t_n), \\ u^{(2)} &\sim g(t_n) + \frac{1}{2}\Delta t g'(t_n) + \frac{1}{4}\Delta t^2 g''(t_n)\,. \end{aligned}$$

Similar modification can by obtained directly for Neumann boundary condition.

2.3 The new SILW method

In this section, we will follow the idea in [15] to get our SILW method for the diffusion equation (2.1). The new type of SILW in [15] decomposes the construction of the ghost point value into "interpolation" and "extrapolation". The interpolation polynomial is obtained based on the interior points near boundary, and then used to value some artificial auxiliary points. A Hermite extrapolation is then constructed based on those auxiliary points values and spatial derivatives at the boundary obtained through the ILW procedure. Finally, ghost point values are approximated by the extrapolation polynomial.

In this paper, we also use "interpolation" and "extrapolation" to get the values of ghost points, but the choice of auxiliary points has a higher degree of freedom and stability analysis indicates that our method yields better results. As the left and right boundaries are completely symmetric for parabolic equations with Dirichlet or Neumann boundary conditions, we will take the left boundary $x = a$ as an example to introduce our SILW method for (2.1) briefly.

2.3.1 The new SILW method for Dirichlet boundary conditions

In this subsection, we discuss the IBVP (2.1) with the Dirichlet boundary condition (2.2). Assume the inner approximation is a d-th order scheme. The new SILW method is:

Algorithm 1. The new SILW method for Dirichlet boundary condition (2.2).

Step 1. Obtain the interpolating polynomial $p(x)$ of degree at most $d-1$ based on the points $\{(x_0, u_0), (x_1, u_1), \cdots, (x_{d-1}, u_{d-1})\}$. Let

$$\begin{aligned} x_{k*} &= a + (\beta + k)\alpha\Delta x, \quad k = 0, 1, 2, \cdots, d - k_d - 1, \\ u_{k*} &= p(x_{k*}), \quad k = 0, 1, 2, \cdots, d - k_d - 1. \end{aligned}$$

Note that we choose $a+\alpha\beta\Delta x$ as the first artificial auxiliary point and the distance between any two adjacent artificial auxiliary points is $\alpha\Delta x$.

Step 2. Construct the extrapolation polynomial $q(x)$ of degree at most $d-1$ to satisfy the following conditions:

$$\begin{aligned} &q^{(2k)}(a) = \partial_x^{(2k)} u|_{x=a} = g_1^{(k)}(t)/c^k, \quad k = 0, 1, 2, \cdots, k_d - 1, \\ &q(x_{k*}) = u_{k*}, \quad k = 0, 1, 2, \cdots, d - k_d - 1. \end{aligned}$$

The second equality in the first row in derived based on the PDE and boundary condition, which is called the ILW procedure.

Step 3. The approximation value at the ghost point x_{-p} is taken as $u_{-p} = q(x_{-p})$.

Here, α, β, k_d are parameters will be determined by stability analysis. In the Dirichlet boundary condition case, only even order derivatives at the boundary $x = a$ can be obtained by the PDE itself through ILW procedure. Note that the SILW method in [15] is a special case of Algorithm 1 with $\beta = 1$.

2.3.2 The new SILW method for Neumann boundary conditions

Same as the procedure in Sect. 2.3.1, we discuss the IBVP (2.1) with the Neumann boundary condition (2.3). Assume the inner approximation is a d-th order scheme. The new SILW method is:

Algorithm 2. The new SILW method for Neumann boundary condition (2.3).

Step 1. Obtain the interpolating polynomial $p(x)$ of degree at most d based on the points $\{(x_0, u_0), (x_1, u_1), \cdots, (x_d, u_d)\}$. Let

$$\begin{aligned} &x_{k*} = a + (\beta + k)\alpha\Delta x, \quad k = 0, 1, 2, \cdots, d - k_d, \\ &u_{k*} = p(x_{k*}), \quad k = 0, 1, 2, \cdots, d - k_d. \end{aligned}$$

Step 2. Construct the extrapolation polynomial $q(x)$ of degree at most d to satisfy the following conditions:

$$\begin{aligned} &q^{(2k+1)}(a) = \partial_x^{(2k+1)} u|_{x=a} = g_3^{(k)}(t)/c^k, \quad k = 0, 1, 2, \cdots, k_d - 1, \\ &q(x_{k*}) = u_{k*}, \quad k = 0, 1, 2, \cdots, d - k_d. \end{aligned}$$

The second equality of the first row in also obtained via the ILW procedure.

Step 3. The approximation value of the ghost point x_{-p} is taken as $u_{-p} = q(x_{-p})$.

Here, α, β, k_d are parameters will be determined by stability analysis. In the Neumann boundary condition case, only odd order derivatives at the boundary $x = a$ can be obtained by the PDE itself through the ILW procedure. Note that the SILW method in [15] is a special case of Algorithm 2 with $\beta = 0.5$.

Clearly, a proper choice of α, β and k_d is the key point to ensure stability for numerical approximations of both Dirichlet and Neumann boundary conditions. We want to find the appropriate value of $\beta \in (0, 5]$ and the corresponding $\alpha \in (0, 5]$ and minimum value of k_d that can ensure stability for all $C_a \in [0, 1)$. Notice that, the smaller the value of k_d, the simpler and less expensive the algorithm becomes. That is, we would like to find $(k_d)_{min}$ which can ensure stability.

3 Stability analysis

In this section, we will apply the Godunov-Ryabenkii method and the eigenvalue spectrum visualization method to analyze stability for both the semi-discrete and fully-discrete schemes. In fact, these two methods yield similar results. The problem considered in this paper consists of two physical boundaries and each boundary can be analyzed separately, that is, stability can be discussed for two quarter-plane problems and a Cauchy problem. As mentioned before, we only perform the stability analysis on the left boundary $x = a$ and the conclusions can be obtained symmetrically for the right boundary. We will give the details of the analysis for the second order scheme at first. The analytical methods can be extended to higher order scheme directly, and the conclusions will be given at the end of this section.

3.1 Semi-discrete schemes

In this subsection, we discuss stability for the semi-discrete schemes. Stability is performed on the quarter-plane problem

$$\begin{cases} u_t = c\, u_{xx}, \quad x \in [a, +\infty), \ t \geq 0, \\ u(x, 0) = u_0(x), \quad x \in [a, +\infty), \end{cases} \tag{3.7}$$

with the Dirichlet boundary $u(a, t) = g_1(t)$, or Neumann boundary condition $u_x(a, t) = g_3(t)$, $t \geq 0$. For convenience, we set $g_1(t) = g_3(t) = 0$. Now let us take the second order scheme (3.8) as an illustration example.

$$\frac{du_j}{dt} = \frac{c}{\Delta x^2} \, (u_{j+1} - 2u_j + u_{j-1}). \tag{3.8}$$

3.1.1 Godunov-Ryabenkii stability analysis

The key point of the Godunov-Ryabenkii method is to determine whether there exists any eigenvalue with positive real part. A complete description of the method can be found in [6, 27].

Let $u_j = e^{st}\phi_j$, scheme (3.8) can be transformed into

$$\widetilde{s}\phi_j = \phi_{j+1} - 2\phi_j + \phi_{j-1}, \tag{3.9}$$

where $\widetilde{s} = s\Delta x^2/c$. In fact, $\widetilde{s}$ can also be regarded as eigenvalue and $\{\phi_j(\widetilde{s})\}_{j=0}^{\infty}$ is the corresponding eigensolution.

Take $\phi_j = \kappa^j$ and plug it into equation (3.9), we can get the characteristic equation as follows,

$$\widetilde{s}\kappa = \kappa^2 - 2\kappa + 1. \tag{3.10}$$

And define

$$f(\kappa) = \kappa^2 - (\widetilde{s} + 2)\kappa + 1. \tag{3.11}$$

In particular, if we take $\kappa = e^{\imath\xi}$, $\xi \in [0, 2\pi]$, (3.10) yields

$$\widetilde{s} = 2(\cos\xi - 1), \tag{3.12}$$

which tells us $\widetilde{s}$ is real and $\widetilde{s} \leq 0$ if $|\kappa| = 1$.

Since $x \in [a, +\infty)$, we are only interested in the roots of the characteristic equation satisfying $|\kappa| < 1$. Same as in [11], if $Re(\widetilde{s}) > 0$, equation (3.12) implies the number of roots for (3.10) with $|\kappa| < 1$ independent of $\widetilde{s}$. We can take any value of $\widetilde{s}$ with $Re(\widetilde{s}) > 0$ to get the number of roots for (3.10) with $|\kappa| < 1$. For instance, taking $\widetilde{s} = 1$, the roots of (3.10) are

$$\kappa_1 \approx 0.381966, \quad \kappa_2 \approx 2.618034.$$

Thus, there is only one root with $|\kappa| < 1$ when $Re(\widetilde{s}) > 0$. Then the general expression of ϕ_j in (3.9) is

$$\phi_j = \sigma\kappa^j. \tag{3.13}$$

• Analysis on the Dirichlet boundary condition

For the second order scheme (3.8), we need the ghost point value u_{-1}. The interpolation polynomial is obtained by $\{(x_0, u_0), (x_1, u_1)\}$. In this case, $d = 2$, we need two conditions in Step 2 of Algorithm 1 to get the extrapolation polynomial $q(x)$ and then the possible minimum value of k_d is 1. Then, the approximate value at the ghost point x_{-1} is

$$u_{-1} = \frac{(C_a - 1)\left((C_a - \alpha\beta + 1)u_0 + (\alpha\beta - C_a)u_1\right)}{\alpha\beta}. \tag{3.14}$$

Plugging (3.13) and (3.14) into (3.8) at $j = 0$ gives us

$$\left(\frac{C_a(C_a - \alpha\beta - 1)}{\alpha\beta}\kappa + \frac{\alpha\beta(C_a + \widetilde{s} + 1) - C_a^2 + 1}{\alpha\beta}\right)\sigma = 0. \tag{3.15}$$

In order to get a nontrivial ϕ_j, we need σ is nonzero and

$$\begin{cases} \dfrac{C_a(C_a - \alpha\beta - 1)}{\alpha\beta}\kappa + \dfrac{\alpha\beta(C_a + \widetilde{s} + 1) - C_a^2 + 1}{\alpha\beta} = 0, \\ f(\kappa) = 0, \\ |\kappa| < 1. \end{cases} \tag{3.16}$$

Here, we take $\beta = 1.37$, $\alpha = 0.24$ as an example. Solving equation (3.16) and taking the maximum value of $Re(\widetilde{s})$ for any $C_a \in [0, 1)$, we plot the results in Fig. 3.1, in which the shaded region is bounded by the maximum value of $Re(\tilde{s})$ and the horizontal axis for different $C_a \in [0, 1)$. Since the region in Fig. 3.1 is below $Re(\tilde{s}) = 0$, this indicates there has no eigenvalue with $Re(\widetilde{s}) > 0$. Thus we can get the conclusion that the semi-discrete second order scheme and the new SILW method with $k_d = 1$, $\beta = 1.37$ and $\alpha = 0.24$ is stable for all $C_a \in [0, 1)$. Notice that in this section $\beta = 1.37$ and $\alpha = 0.24$ is taken as an example to demonstrate the results, for other choices of β and α , we can perform the same procedure and get the corresponding results.

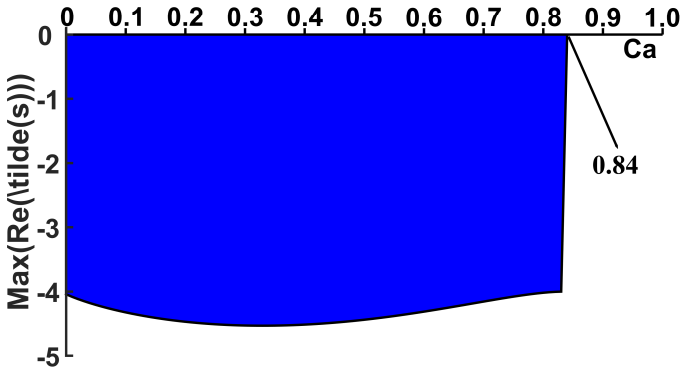

Fig. 3.1: Godunov-Ryabenkii analysis on the right-plane problem with Dirichlet boundary conditions: Second order semi-discrete scheme and the new SILW method with $k_d = 1$, $\beta = 1.37$ and $\alpha = 0.24$.

Furthermore, taking $\beta = 1$, we can get that there has no eigenvalue with positive real part or the maximum value of $Re(\widetilde{s})$ is 0 for any value of $\alpha \in (0, 5]$ and $C_a \in [0, 1)$. That means for $\beta = 1$, we can take any value of $\alpha \in (0, 5]$, the second order semi-discrete scheme with the new SILW method with $k_d = 1$ is stable for all $C_a \in [0, 1)$.

• **Analysis on the Neumann boundary condition**

In this case, the interpolation polynomial $p(x)$ is obtained by $\{(x_0, u_0),\ (x_1, u_1),\ (x_2, u_2)\}$. Without loss of generality, we set $g_3(t) = 0$. And the possible minimum value of k_d is $k_d = 1$.

As before, the characteristic equation is (3.10), the eigenvalue problem is (3.9) and the general expression of ϕ_j is (3.13). When $k_d = 1$, the approximate values at the ghost point x_{-1} is

$$\begin{aligned} u_{-1} = &-\frac{\alpha^2\beta(\beta+1)(2C_a+3)+(C_a-1)^2(2C_a+3)-\alpha(2\beta+1)(2C_a^2+C_a+3)}{2(\alpha+2\alpha\beta)}u_0 \\ &+\frac{2\alpha^2\beta(\beta+1)(C_a+1)+2(C_a-1)^2(C_a+1)-\alpha(2\beta+1)(2C_a^2+1)}{\alpha+2\alpha\beta}u_1 \\ &-\frac{\alpha^2\beta(\beta+1)(2C_a+1)+(C_a-1)^2(2C_a+1)-\alpha(2\beta+1)(2C_a^2-C_a+1)}{2(\alpha+2\alpha\beta)}u_2. \end{aligned} \tag{3.17}$$

Plug (3.17) and (3.13) into (3.8) at $j = 0$ and we then have

$$(b_2\kappa^2 + b_1\kappa + b_0)\sigma = 0, \tag{3.18}$$

where

$$\begin{aligned} b_0 &= \frac{\alpha^2\beta(\beta+1)(2C_a+3)+(C_a-1)^2(2C_a+3)-\alpha(2\beta+1)(2C_a^2+C_a-1-2\widetilde{s})}{2(\alpha+2\alpha\beta)}, \\ b_1 &= -\frac{2(-\alpha(2\beta+1)C_a^2+\alpha^2\beta(\beta+1)(C_a+1)+(C_a-1)^2(C_a+1))}{\alpha+2\alpha\beta}, \\ b_2 &= \frac{\alpha^2\beta(\beta+1)(2C_a+1)+(C_a-1)^2(2C_a+1)-\alpha(2\beta+1)(2C_a^2-C_a+1)}{2(\alpha+2\alpha\beta)}. \end{aligned}$$

In order to get a nontrivial ϕ_j, we need σ is nonzero and

$$\begin{cases} b_2\kappa^2 + b_1\kappa + b_0 = 0, \\ f(\kappa) = 0, \\ |\kappa| < 1. \end{cases} \tag{3.19}$$

As before, we take $\alpha = 0.24$, $\beta = 1.37$ as one example. Solving equation (3.19) and taking the maximum value of $Re(\widetilde{s})$, the results are shown in Fig. 3.2, indicating the semi-discrete second order scheme for the Neumann boundary problem with the new SILW method with $k_d = 1$, $\beta = 1.37$ and $\alpha = 0.24$ is stable for all $C_a \in [0, 1)$.

As an special case in [15], we take $\beta = 0.5$. For any fixed $\alpha \in (0, 5]$, we look at the maximum value of $Re(\widetilde{s})$ for $C_a \in [0, 1)$, and the results are shown in Fig. 3.3, indicating the semi-discrete second order scheme for the Neumann boundary problem with the new SILW method with $k_d = 1$ and $\beta = 0.5$ is stable for all $\alpha \in (0, 5]$, $C_a \in [0, 1)$.

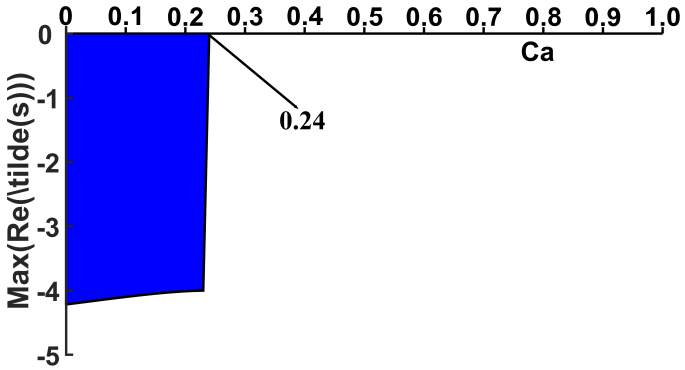

Fig. 3.2: Godunov-Ryabenkii analysis on the right-plane problem with Neumann boundary conditions: Second order semi-discrete scheme and the new SILW method with $k_d = 1$, $\beta = 1.37$ and $\alpha = 0.24$.

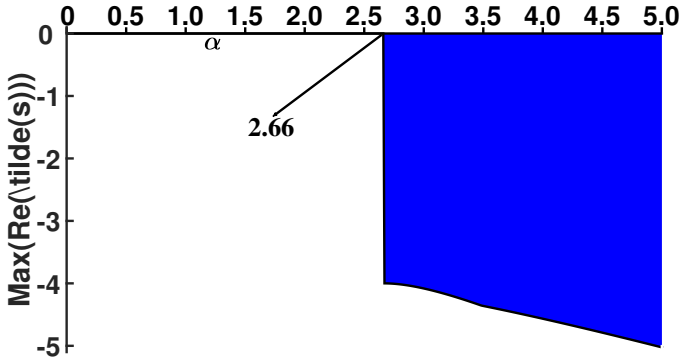

Fig. 3.3: Godunov-Ryabenkii analysis on the right-plane problem with Neumann boundary conditions: Second order semi-discrete scheme and the new SILW method with $k_d = 1$, $\beta = 0.5$ and $\alpha \in (0, 5]$.

3.1.2 Eigenvalue spectrum visualization

For the higher order schemes, the Godunov-Ryabenkii method leads to heavy calculations. So we use an alternative eigenvalue spectrum visualization method [32] which is easier to carry out to analyze stability. And our analysis results can be validated by numerical experiments in the next section.

As demonstrate in [32], the eigenvalue spectrum visualization method needs to consider stability with the two boundaries together. For simplicity, we set $g_1(t) = g_2(t) = g_3(t) = g_4(t) = 0$. The semi-discrete schemes can be transformed into a matrix-vector form as

$$\frac{d\vec{U}}{dt} = \frac{c}{\Delta x^2} Q\vec{U}, \tag{3.20}$$

where $\vec{U} = (u_0, u_1, \cdots, u_N)^T$ and Q is a matrix. This system contains the chosen interior scheme and numerical boundary conditions.

Taking $u(x,t) = e^{st}v(x)$, (3.20) turns to

$$\tilde{s}\vec{U} = Q\vec{U}. \tag{3.21}$$

In this case, we needs to focus on the "fixed" eigenvalues, namely those eigenvalues which are equal (subject to a negligible difference due to round-off errors and eigenvalue solver accuracy) for different values of grid number N. Similar to the Godunov-Ryabenkii method, there may exist more than one "fixed" eigenvalue of the matrix Q, and we concentrate on the maximum value of the real part of those "fixed" eigenvalues. Here, we also take the second order scheme (3.8) as an example to explain this method in detail.

Similar to the analysis in Sect. 3.1.1, we only analyze the stability of the right-plane problem. For the second order scheme (3.8), the ghost point u_{-1} is obtained by the new SILW method and we set $u_{N+1} = 0$ to eliminate the influence to stability from the right boundary. Then we can get the the matrix-vector form (3.20).

• **Analysis on Dirichlet boundary condition**

As before, we choose $k_d = 1$, $\beta = 1.37$ and $\alpha = 0.24$ and use different values of N to find the largest real part of all the "fixed" eigenvalues. The results are shown in Fig. 3.4. Comparing Fig. 3.1 and Fig. 3.4, we can see they are almost the same. So the eigenvalue spectrum visualization could be an alternative approach to analyze stability. Furthermore, take $\beta = 1$. We can get the similar results as in Sect. 3.1.1 that the maximum value of $Re(\widetilde{s})$ is not larger than 0 for all $\alpha \in (0, 5]$ and $C_a \in [0, 1)$.

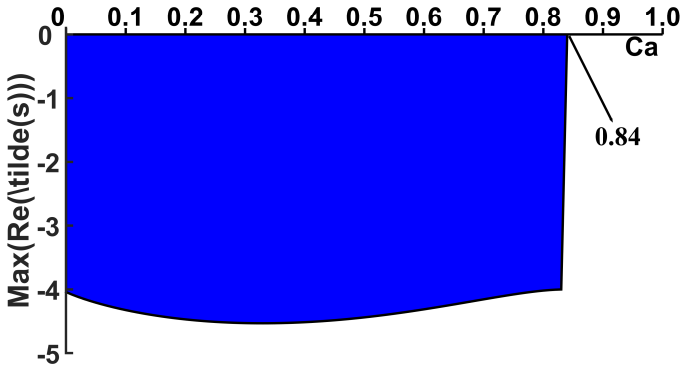

Fig. 3.4: Eigenvalue spectrum visualization on the right-plane problem with Dirichlet boundary conditions: Second order semi-discrete scheme and the new SILW method with $k_d = 1$, $\beta = 1.37$ and $\alpha = 0.24$.

• **Analysis on the Neumann boundary condition**

For the Neumann boundary condition, the results of $k_d = 1$, $\beta = 1.37$ and $\alpha = 0.24$ are displayed in Fig. 3.5 and the results of $\beta = 0.5$ are displayed in Fig. 3.6. It is observed that Fig. 3.2 and Fig. 3.5, Fig. 3.3 and Fig. 3.6 are almost the same. So we can rely on the eigenvalue spectrum visualization to analyze stability and the results demonstrate that for the Neumann boundary condition, the second order semi-discrete scheme and the new SILW method with $k_d = 1$, $\beta \in (0, 5]$ and $\alpha \in (0, 5]$ is stable for all $C_a \in [0, 1)$. Note that as the eigenvalue spectrum visualization is not as accurate as the Godunov-Ryabenkii analysis since Fig. 3.3 and Fig. 3.6 have slight difference, but under the same circumstances, these two methods show the same stability results.

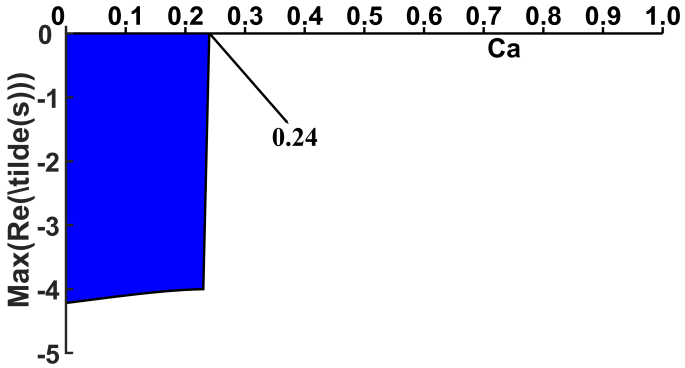

Fig. 3.5: Eigenvalue spectrum visualization on the right-plane problem with Neumann boundary conditions: Second order semi-discrete scheme and the new SILW method with $\beta = 1.37$, $\alpha = 0.24$ and $k_d = 1$.

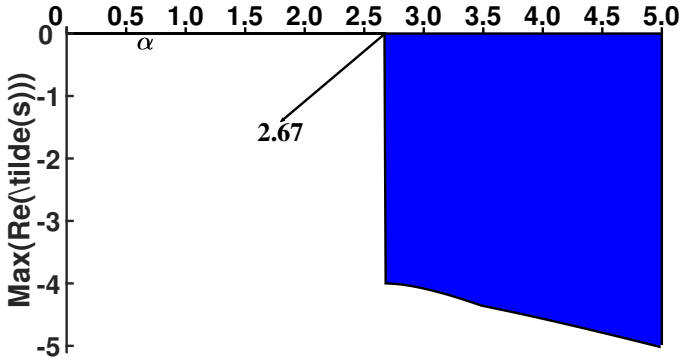

Fig. 3.6: Eigenvalue spectrum visualization on the right-plane problem with Neumann boundary conditions: Second order semi-discrete scheme and the new SILW method with $\beta = 0.5$, $k_d = 1$ and $\alpha \in (0, 5]$.

3.2 Fully-discrete Schemes

For the semi-discrete scheme (2.5), we use the third order TVD Runge-Kutta method (2.6) as the time discretization to get the fully-discrete scheme. The detailed procedure can be found in [13, 14].

For the fully-discrete scheme, an eigensolution is defined in the form of $u_j^{n+1} = z(\mu)u_j^n$ with $\mu = s\Delta t = \tilde{s}\lambda_{cfl}$, $\lambda_{cfl} = \dfrac{c\Delta t}{\Delta x^2}$ and $|z(\mu)| > 1$, where

$$z(\mu) = 1 + \mu + \frac{\mu^2}{2} + \frac{\mu^3}{6}. \tag{3.22}$$

Here, $\tilde{s}$ is an eigenvalue of the semi-discrete scheme and $z(\mu)$ is the eigenvalue of the fully-discrete scheme. In the fully-discrete cases, the scheme is unstable if such candidate eigensolution exists.

Denote $(\lambda_{cfl})_{max}$ as the largest CFL number of the fully-discrete scheme for the Cauchy problems. As in [11, 12, 13, 14, 16], we use $(\lambda_{cfl})_{max}$ as our CFL number when verifying the stability of the fully-discrete numerical schemes for the initial-boundary value problem. This means we do not want the boundary treatment to affect the CFL number of interior schemes for the corresponding Cauchy problem. The detailed procedure to find $(\lambda_{cfl})_{max}$ can be found in [14] and we just list the values for the schemes in Sect. 2.1 in Tab. 3.1.

Tab. 3.1: $(\lambda_{cfl})_{\max}$ for different schemes.

Scheme	2nd order	4th order	6th order	8th order	10th order
$(\lambda_{cfl})_{max}$	0.628	0.471	0.415	0.386	0.368

3.2.1 Godunov-Ryabenkii stability analysis

For the Godunov-Ryabenkii stability analysis, $\tilde{s}$ is the eigenvalue obtained in the semi-discrete case and

$$\mu = s\Delta t = (\lambda_{cfl})_{max}\tilde{s}.$$

Here, we only consider the second order scheme.

• **Analysis on Dirichlet boundary condition**

As in Sect. 3.1.1, there may exist more than one eigenvalue $\tilde{s}$. We focus on the maximum value of $|z(\mu)|$ defined in equation (3.22). The results of $\beta = 1.37$ and $\alpha = 0.24$ are shown in Fig. 3.7, and those of $\beta = 1$ and $\alpha \in (0, 5]$ are shown in Fig. 3.8. The shaded regions are bounded by the the maximum value of $|z(\mu)|$ and the horizontal axis. The

region above $|z(\mu)| = 1$ indicates instability. It is observed from Fig. 3.7 that for the Dirichlet boundary problem, the second order fully-discrete scheme and the new SILW method with $k_d = 1$, $\beta = 1.37$ and $\alpha = 0.24$ is stable for $C_a \in [0.83, 1)$. Thus, this choice of parameters can not been utilized in our numerical simulation. And Fig. 3.8 shows that for $\beta = 1.0$ and $\alpha \in [0.5, 5]$, the scheme is stable for all $C_a \in [0, 1)$, indicating that this is a reasonable parameter selection area.

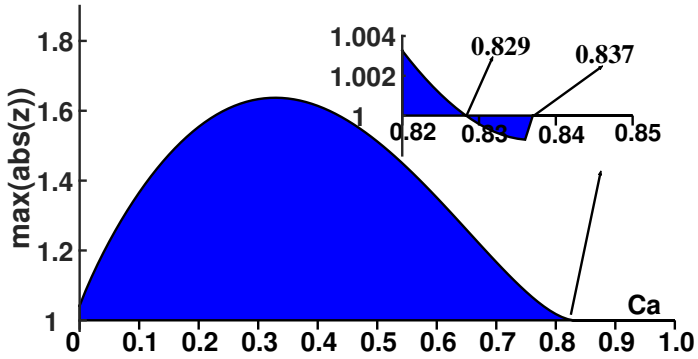

Fig. 3.7: Godunov-Ryabenkii analysis on the right-plane problem with Dirichlet boundary conditions: Second order fully-discrete scheme and the new SILW method with $k_d = 1$, $\beta = 1.37$ and $\alpha = 0.24$.

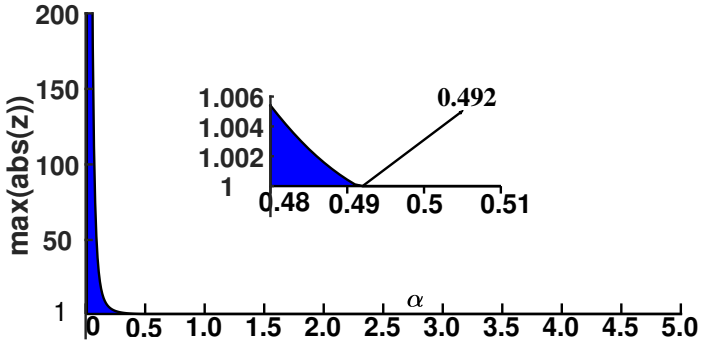

Fig. 3.8: Godunov-Ryabenkii analysis on the right-plane problem with Dirichlet boundary conditions: Second order fully-discrete scheme and the new SILW method with $k_d = 1$, $\beta = 1.0$ and $\alpha \in (0, 5]$.

- **Analysis on Neumann boundary condition**

The results for the Neumann boundary condition are shown in Fig. 3.9 and Fig. 3.10. Fig. 3.9 indicates that for the second order fully-discrete scheme and the new SILW method with $k_d = 1$, if we take $\beta = 1.37$ and $\alpha = 0.24$, the scheme is only

stable for $C_a \in [0.23, 1.0)$. And Fig. 3.10 indicates that if set $\beta = 0.5$, we can take $\alpha \in [0.65, 1.9]$ to get a stable scheme for all $C_a \in [0, 1)$.

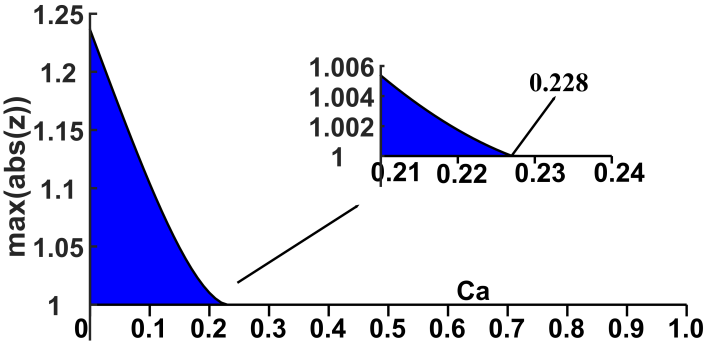

Fig. 3.9: Godunov-Ryabenkii analysis on the right-plane problem with Neumann boundary conditions: Second order fully-discrete scheme and the new SILW method with $k_d = 1$, $\alpha = 0.24$ and $\beta = 1.37$.

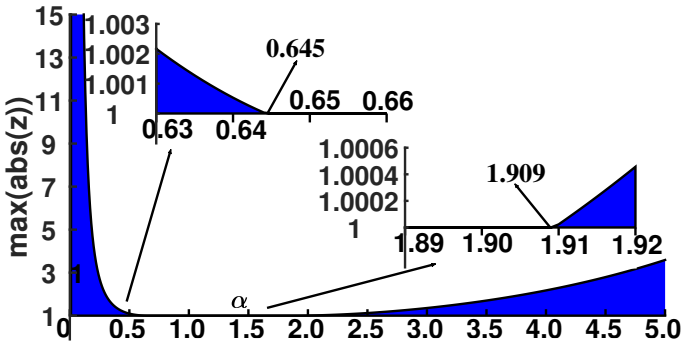

Fig. 3.10: Godunov-Ryabenkii analysis on the right-plane problem with Neumann boundary conditions: Second order fully-discrete scheme and the new SILW method with $k_d = 1$, $\beta = 0.5$ and $\alpha \in (0, 5]$.

3.2.2 Eigenvalue spectrum visualization

In this subsection, the eigenvalue spectrum visualization method is used to get the stability results for the second order fully-discrete scheme. By using the third order TVD Runge-Kutta method, the matrix formulation (3.20) can be transformed to the fully-discrete scheme

$$\vec{U}^{n+1} = G\vec{U}^n, \quad G = I + \frac{c\Delta t}{\Delta x^2}Q + \frac{1}{2}\Big(\frac{c\Delta t}{\Delta x^2}Q\Big)^2 + \frac{1}{6}\Big(\frac{c\Delta t}{\Delta x^2}Q\Big)^3, \tag{3.23}$$

where I is the identity matrix. Same as in [13], we need all the eigenvalues of G to lie inside the unit circle. i.e. $|z(\mu)| \leq 1$, to ensure stability of the fully-discrete approximation.

• **Analysis on Dirichlet boundary condition**

The maximum values of $|z(\mu)|$ as defined in equation (3.22) are shown in Fig. 3.11 and Fig. 3.12. It can be seen that Fig. 3.7 is similar to Fig. 3.11, and Fig. 3.8 is similar to Fig. 3.12. Thus, we can rely on the eigenvalue spectrum visualization to get stability results.

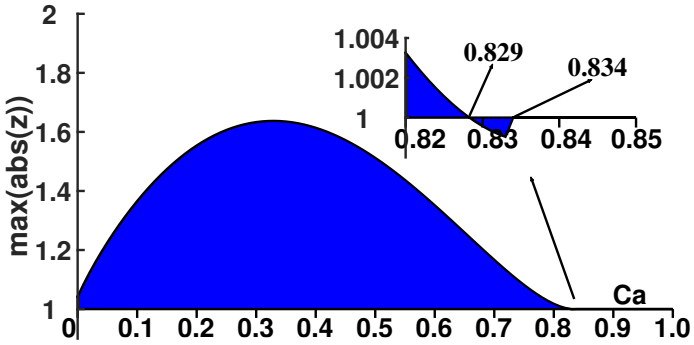

Fig. 3.11: Eigenvalue spectrum visualization on the right-plane problem with Dirichlet boundary conditions: Second order fully-discrete scheme and the new SILW method with $k_d = 1$, $\beta = 1.37$ and $\alpha = 0.24$.

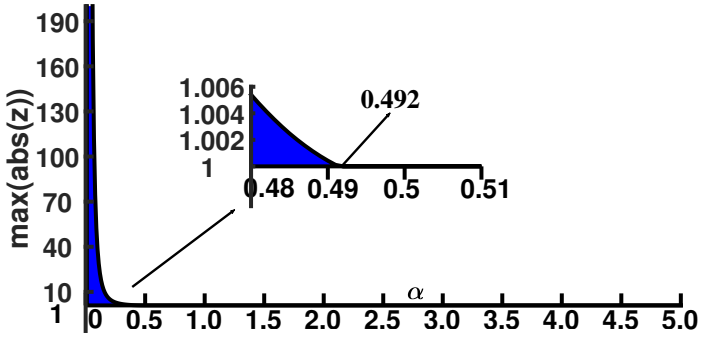

Fig. 3.12: Eigenvalue spectrum visualization on the right-plane problem with Dirichlet boundary conditions: Second order fully-discrete scheme and the new SILW method with $k_d = 1$, $\beta = 1$ and and $\alpha \in (0, 5]$.

• **Analysis on Neumann boundary condition**

The results of the Neumann boundary problem are provided in Fig. 3.13 and Fig. 3.14. Comparing Fig. 3.9 with Fig. 3.13 and Fig. 3.10 with Fig. 3.14 , we can see that

they are almost the same. By carefully observing, we can find that Fig. 3.9 and Fig. 3.13 have minor difference, this is due to the fact that eigenvalue spectrum visualization method is not exactly as Godunov-Ryabenkii analysis, but they have the same stability results. Thus we can use the eigenvalue spectrum visualization to get stability results for the remaining high order schemes in Sect. 2.1.

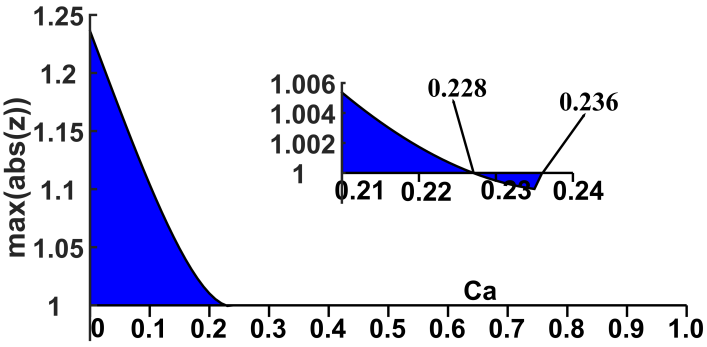

Fig. 3.13: Eigenvalue spectrum visualization on the right-plane problem with Neumann boundary conditions: Second order fully-discrete scheme and the new SILW method with $k_d = 1$, $\beta = 1.37$ and $\alpha = 0.24$.

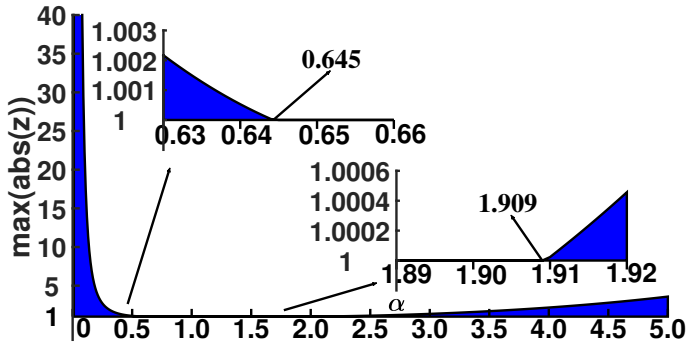

Fig. 3.14: Eigenvalue spectrum visualization on the right-plane problem with Neumann boundary conditions: Second order fully-discrete scheme and the new SILW method with $k_d = 1$, $\beta = 0.5$ and $\alpha \in (0, 5]$.

3.3 High order schemes

The method in [15] is a special case of the new SILW method in this paper, which corresponding to $\beta = 1.0$ for the Dirichlet boundary problem and $\beta = 0.5$ for the Neumann boundary problem. Stability analysis results of this special case are displayed

in Tab. 3.2 for the fully-discrete schemes, showing the minimum value of k_d (denoted by $(k_d)_{min}$) with appropriate range of α that can guarantee stability for all $C_a \in [0, 1)$.

Tab. 3.2: $(k_d)_{min}$ and range of α for different schemes.

Scheme	Dirichlet boundary condition with $\beta = 1.0$		Neumann boundary condition with $\beta = 0.5$	
	$(k_d)_{min}$	α	$(k_d)_{min}$	α
2nd order	1	[0.5,5.0]	1	[0.65,1.90]
4th order	1	[0.74,2.48]	1	[0.99,1.33]
6th order	1	[0.89,1.17]	2	[1.97,3.75]
8th order	2	[0.82,1.22]	2	[2.14,2.15]
10th order	2	[0.89,0.99]	–	–

Compared with the method in [15], the new SILW method in this paper has extended and improved the selection method of artificial auxiliary points. For $\beta \in (0, 5]$, we would like to search if there have appropriate range of $\alpha \in (0, 5]$ and $(k_d)_{min}$ that can ensure stability for all $C_a \in [0, 1)$, the results can be found in Tab. 3.3 for the fully-discrete schemes.

Comparing Tab. 3.2 with Tab. 3.3, it is clearly observed that our method reveals better results than the method in [15]. For example, for the Neumann boundary condition problem with the sixth order scheme, the method in [15] needs $(k_d)_{min} = 2$ to get a stable scheme, but our method can get a stable scheme for all $C_a \in [0, 1)$ with $(k_d)_{min} = 1$. The method in [15] fails to get a stable scheme in the case of Neumann boundary condition with tenth order scheme, while our the method can get a stable scheme with $(k_d)_{min} = 4$ with proper choice of α, β.

For some different values of β, the corresponding range of α that can ensure stability for all $C_a \in [0, 1)$ can be found in Tab. A.18 - A.22 in Appendix A.

4 Numerical examples

In this section, we present some numerical examples to demonstrate that our method is stable and high accuracy with the results in Tab. 3.3. These numerical tests also indicate the obtained stability results are sufficient for stability of the boundary treatments.

Tab. 3.3: $(k_d)_{min}$ and range of β for different schemes.

Scheme	Dirichlet boundary condition		Neumann boundary condition	
	$(k_d)_{min}$	β	$(k_d)_{min}$	β
2nd order	1	[0.10,5.0]	1	[0.01,5.0]
4th order	1	[0.10,5.0]	1	[0.02,0.60]
6th order	1	[0.39,5.0]	1	[0.03,0.40]
8th order	2	[0.38,5.0]	2	[0.48,0.70]
10th order	2	[0.46,5.0]	4	[1.07,1.94]

Consider the following problem

$$\begin{cases} u_t = u_{xx}, \quad x \in (1.5, 3.5),\ t \geq 0, \\ u(x,0) = \sin(x), \quad x \in (1.5, 3.5). \end{cases} \tag{4.24}$$

The corresponding Dirichlet boundary conditions are

$$\begin{cases} u(1.5,t) = e^{-t}\sin(1.5), \\ u(3.5,t) = e^{-t}\sin(3.5). \end{cases} \tag{4.25}$$

While the corresponding Neumann boundary conditions are

$$\begin{cases} u_x(1.5,t) = e^{-t}\cos(1.5), \\ u_x(3.5,t) = e^{-t}\cos(3.5). \end{cases} \tag{4.26}$$

For both boundary conditions, the exact solution is

$$u(x,t) = e^{-t}\sin(x).$$

Without special declaration, the time step size Δt is chosen as

$$\Delta t = (\lambda_{cfl})_{max}\Delta x^2, \tag{4.27}$$

and $(\lambda_{cfl})_{max}$ is the maximum CFL number shown in Tab. 3.1.

4.1 Results for Dirichlet boundary condition

Numerical results of boundary treatments for equation (4.24) with the Dirichlet boundary condition (4.25) are shown in this subsection.

• **The second order scheme**

Firstly, take $\beta = 1.0$ and $(k_d)_{min} = 1$. In this case, α should between $[0.5, 5.0]$ to guarantee a stable scheme for all $C_a \in [0, 1)$, $C_b \in [0, 1)$. Fig. 4.15 shows the scheme is unstable with $\alpha = 0.49$ and is stable with $\alpha = 0.5$ for $C_a = C_b = 0.46$. Tab. 4.4 demonstrates that the scheme is stable and shows the designed second order accuracy with different C_a and C_b for $\alpha = 3.3$ and $\beta = 2.82$, which lie in the range in Tab. A.18.

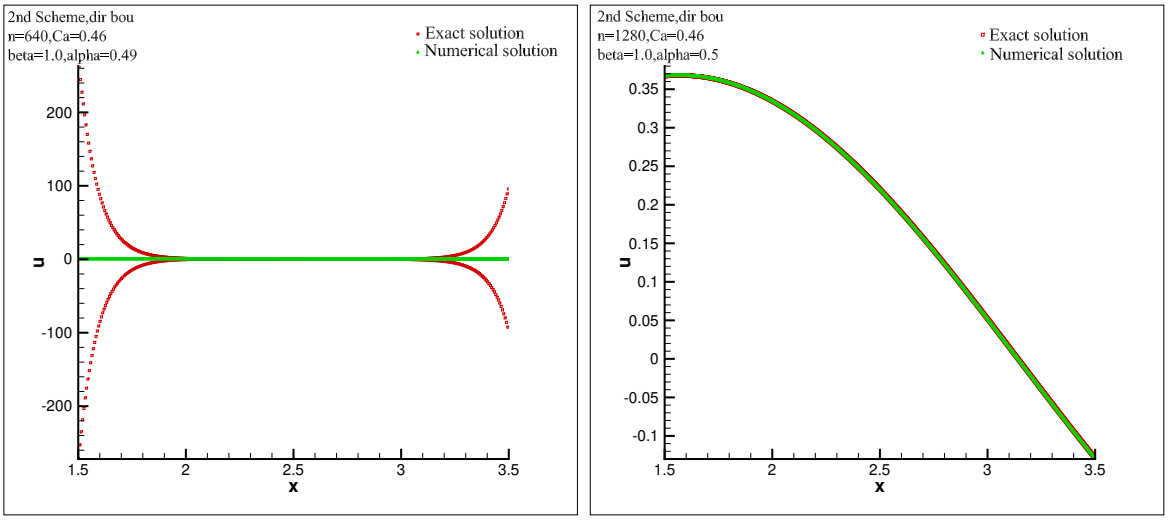

Fig. 4.15: The second order scheme and the new SILW method with $\beta = 1.0$, $k_d = 1$, $C_a = C_b = 0.46$, $t_{end} = 1.0$ and CFL condition (4.27). Left: $\alpha = 0.49$ and $N = 640$; Right: $\alpha = 0.50$ and $N = 1280$.

Tab. 4.4: The second order scheme with $\beta = 2.82$, $\alpha = 3.3$, $k_d = 1$, $t_{end} = 1.0$ and CFL condition (4.27) for the heat equation with Dirichlet boundary conditions.

N	$C_a = 10^{-8}$, $C_b = 10^{-8}$				$C_a = 1 - 10^{-8}$, $C_b = 1 - 10^{-8}$			
	L^2 *error*	order	L^∞ *error*	order	L^2 *error*	order	L^∞ *error*	order
40	7.184E-04	–	8.303E-04	–	2.552E-05	–	2.567E-05	–
80	1.777E-04	2.016	2.072E-04	2.002	6.695E-06	1.931	6.737E-06	1.930
160	4.419E-05	2.007	5.178E-05	2.001	1.715E-06	1.965	1.726E-06	1.965
320	1.102E-05	2.004	1.294E-05	2.000	4.342E-07	1.982	4.369E-07	1.982
640	2.751E-06	2.002	3.234E-06	2.000	1.092E-07	1.991	1.099E-07	1.991
1280	6.874E-07	2.001	8.090E-07	2.000	2.739E-08	1.996	2.756E-08	1.996

• **The fourth order scheme**

Consider $\beta = 1.0$ and $(k_d)_{min} = 1$, then α can be chosen as $\alpha \in [0.74, 2.48]$ to get a stable scheme for all $C_a \in [0, 1)$, $C_b \in [0, 1)$. Figure 4.16 and Figure 4.17 give the

stability and instability results. Table 4.5 shows the fourth order with small and large C_a and C_b if the scheme is stable.

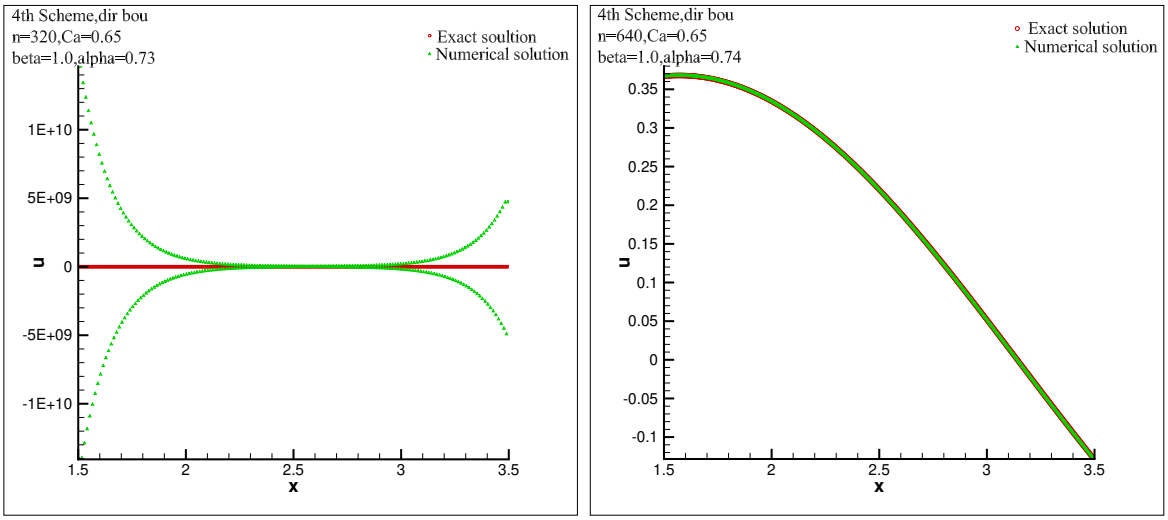

Fig. 4.16: The fourth order scheme and the new SILW method with $\beta = 1.0$, $k_d = 1$, $C_a = C_b = 0.65$, $t_{end} = 1.0$ and the CFL condition (4.27). Left: $\alpha = 0.73$ and $N = 320$; Right: $\alpha = 0.74$ and $N = 640$.

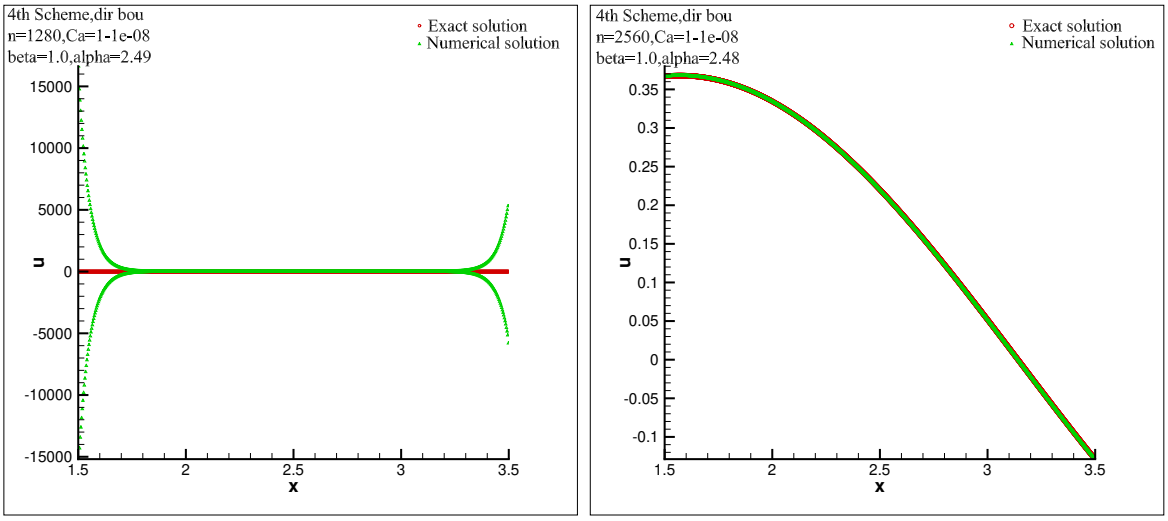

Fig. 4.17: The fourth order scheme and the new SILW method with $\beta = 1.0$, $k_d = 1$, $C_a = C_b = 1 - 10^{-8}$, $t_{end} = 1.0$ with CFL condition (4.27). Left: $\alpha = 2.49$ and $N = 1280$; Right: $\alpha = 2.48$ and $N = 2560$.

- **The sixth order scheme**

Take $\beta = 1.0$ and $(k_d)_{min} = 1$. To get a stable scheme for all $C_a \in [0, 1)$, $C_b \in [0, 1)$, the corresponding range of α is $\alpha \in [0.89, 1.17]$. Fig. 4.18 and 4.19 show the stability

Tab. 4.5: The fourth order scheme with $\beta = 3.91$, $\alpha = 0.4$, $k_d = 1$, $t_{end} = 1.0$ and CFL condition (4.27) for the heat equation with Dirichlet boundary conditions. .

N	$C_a = 10^{-8}$, $C_b = 10^{-8}$				$C_a = 1 - 10^{-8}$, $C_b = 1 - 10^{-8}$			
	L^2 *error*	order	L^∞ *error*	order	L^2 *error*	order	L^∞ *error*	order
40	4.302E-07	–	5.439E-07	–	2.215E-07	–	2.572E-07	–
80	2.626E-08	4.034	3.397E-08	4.001	1.522E-08	3.864	1.782E-08	3.851
160	1.621E-09	4.018	2.122E-09	4.001	9.982E-10	3.930	1.175E-09	3.923
320	1.007E-10	4.001	1.326E-10	4.001	6.392E-11	3.965	7.540E-11	3.962
640	6.274E-12	4.005	8.284E-12	4.000	4.045E-12	3.982	4.775E-12	3.981
1280	3.915E-13	4.002	5.177E-13	4.000	2.544E-13	3.991	3.005E-13	3.990

and instability results. The numerical results in Tab. 4.6 shows that the scheme is stable and can reach the designed high order.

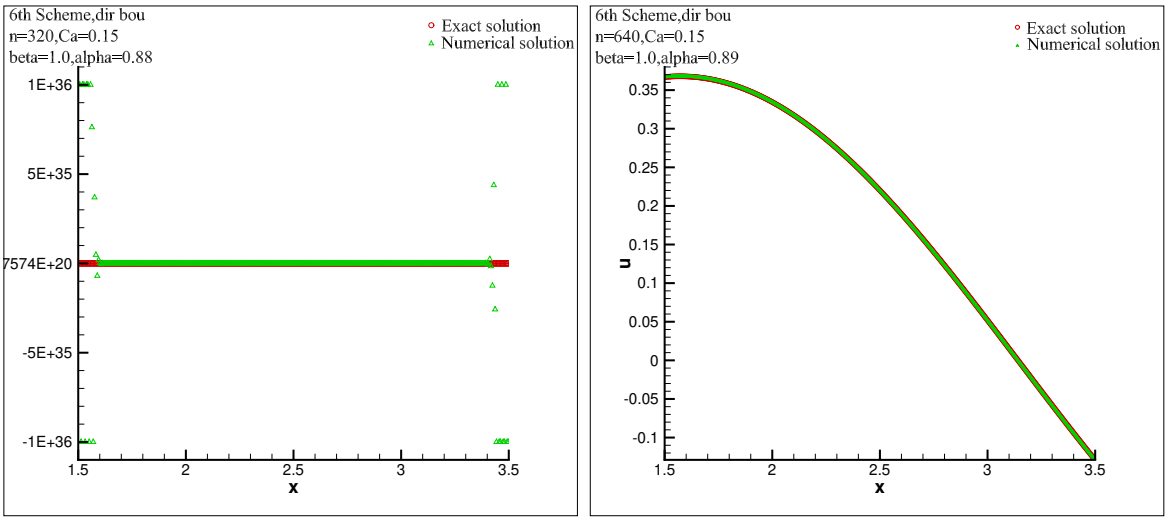

Fig. 4.18: The sixth order scheme and the new SILW method with $\beta = 1.0$, $k_d = 1$, $C_a = C_b = 0.15$, $t_{end} = 1.0$ and CFL condition (4.27). Left: $\alpha = 0.88$ and $N = 320$; Right: $\alpha = 0.89$ and $N = 640$.

- **The eighth order scheme**

Again, take $\beta = 1.0$ and $(k_d)_{min} = 2$. In order to get a stable scheme for all $C_a \in [0, 1)$, $C_b \in [0, 1)$, α can be choose as $\alpha \in [0.82, 1.22]$. Fig. 4.20 shows the scheme is unstable with $\alpha = 0.81$ but stable with $\alpha = 0.82$ for $\beta = 1.0$, $k_d = 2$, $C_a = C_b = 0.78$. Fig. 4.21 shows the scheme is unstable with $\alpha = 1.23$ but stable with $\alpha = 1.22$ for $\beta = 1.0$, $k_d = 2$, $C_a = C_b = 0.01$. Tab. 4.7 shows that we can get the sixth order with small and large C_a

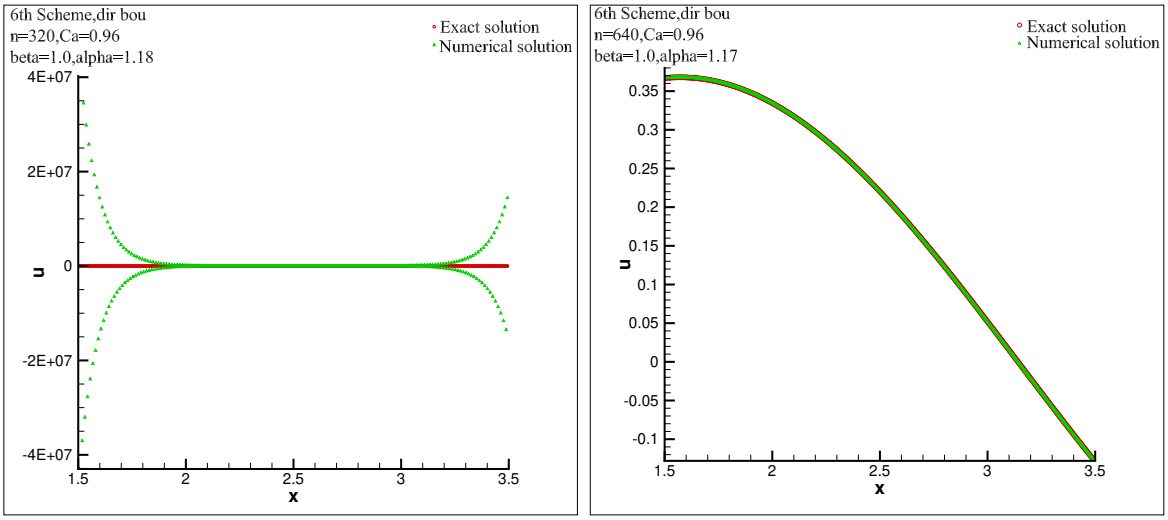

Fig. 4.19: The sixth order scheme and the new SILW method with $\beta = 1.0$, $k_d = 1$, $C_a = C_b = 0.96$, $t_{end} = 1.0$ and CFL condition (4.27). Left: $\alpha = 1.18$ and $N = 320$; Right: $\alpha = 1.17$ and $N = 640$.

Tab. 4.6: The sixth order scheme with $\beta = 0.9$, $\alpha = 1.1$, $k_d = 1$, $t_{end} = 1.0$ and CFL condition (4.27) for the heat equation with Dirichlet boundary conditions.

N	$C_a = 10^{-8}$, $C_b = 10^{-8}$				$C_a = 1 - 10^{-8}$, $C_b = 1 - 10^{-8}$			
	L^2 *error*	order	L^∞ *error*	order	L^2 *error*	order	L^∞ *error*	order
40	6.678E-10	–	7.589E-10	–	3.757E-10	–	4.664E-10	–
80	1.018E-11	6.036	1.196E-11	5.987	6.661E-12	5.817	8.447E-12	5.787
160	1.570E-13	6.019	1.876E-13	5.995	1.110E-13	5.907	1.422E-13	5.893
320	2.437E-15	6.009	2.939E-15	5.996	1.792E-15	5.953	2.306E-15	5.946
640	3.795E-17	6.005	4.599E-17	5.998	2.846E-17	5.976	3.671E-17	5.973
1280	5.920E-19	6.002	7.190E-19	5.999	4.483E-19	5.988	5.790E-19	5.987

and C_b for suitable α and β. Moreover, if take the time step as

$$\Delta t = (\lambda_{cfl})_{max} \Delta x^{8/3}, \tag{4.28}$$

we can get Tab. 4.8, indicating the designed eighth order accuracy.

- **The tenth order scheme**

Take $\beta = 1.0$, $(k_d)_{min} = 2$ and $\alpha \in [0.89, 0.99]$, the scheme is stable for all $C_a \in [0, 1)$, $C_b \in [0, 1)$. Fig. 4.22 and 4.23 show the stability and instability results. Tab. 4.9 indicates the corresponding sixth order with appropriate α and β. In additional, taking step size Δt as

$$\Delta t = (\lambda_{cfl})_{max} \Delta x^{10/3} \tag{4.29}$$

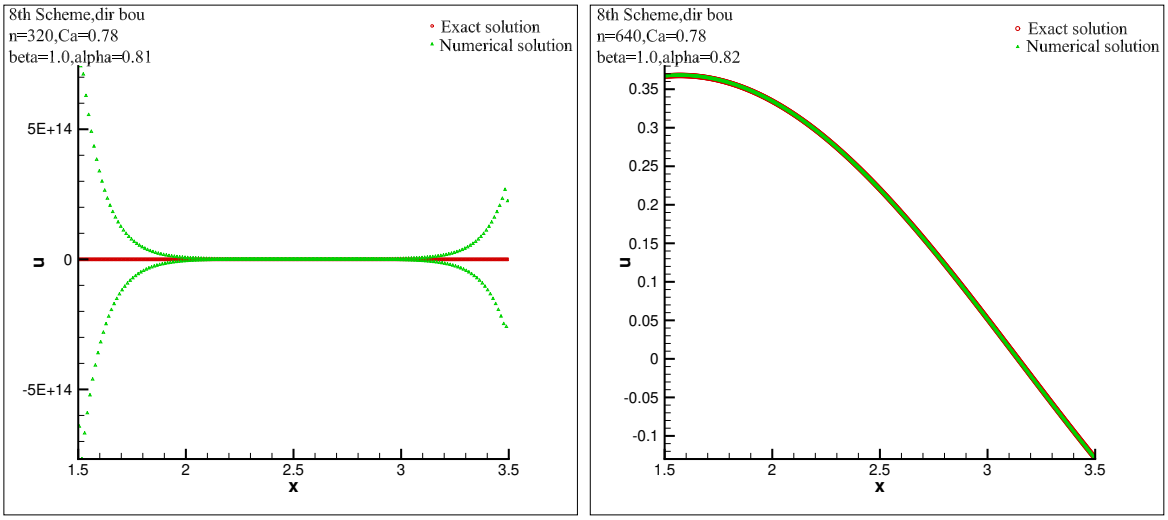

Fig. 4.20: The eighth order scheme and the new SILW method with $\beta = 1.0$, $k_d = 2$, $C_a = C_b = 0.78$, $t_{end} = 1$ and CFL condition (4.27). Left: $\alpha = 0.81$ and $N = 320$; Right: $\alpha = 0.82$ and $N = 640$.

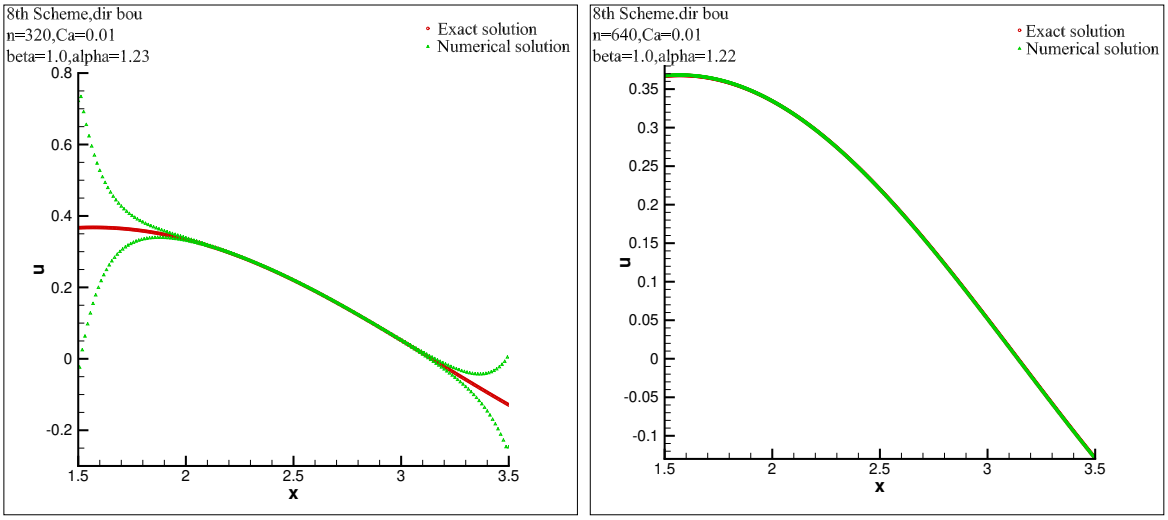

Fig. 4.21: The eighth order scheme and the new SILW method with $\beta = 1.0$, $k_d = 2$, $C_a = C_b = 0.01$, $t_{end} = 1.0$ and CFL condition (4.27). Left: $\alpha = 1.23$ and $N = 320$; Right: $\alpha = 1.22$ and $N = 640$.

can provided tenth order accuracy, as shown in Tab. 4.10.

4.2 Results for Neumann boundary condition

Numerical results of boundary treatments for equation (4.24) with the boundary condition (4.26) are shown in this subsection.

Tab. 4.7: The eighth order scheme with $\beta = 1.92$, $\alpha = 0.59$, $k_d = 2$, $t_{end} = 1.0$ and CFL condition (4.27) for the heat equation with Dirichlet boundary conditions.

N	$C_a = 10^{-8}$, $C_b = 10^{-8}$				$C_a = 1 - 10^{-8}$, $C_b = 1 - 10^{-8}$			
	L^2 *error*	order	L^∞ *error*	order	L^2 *error*	order	L^∞ *error*	order
40	5.020E-12	–	5.055E-12	–	3.839E-12	–	3.855E-12	–
80	7.889E-14	5.992	7.939E-14	5.993	6.842E-14	5.810	6.883E-14	5.808
160	1.234E-15	5.998	1.242E-15	5.998	1.147E-15	5.898	1.154E-15	5.898
320	1.929E-17	6.000	1.941E-17	6.000	1.859E-17	5.948	1.870E-17	5.947
640	3.014E-19	6.000	3.033E-19	6.000	2.958E-19	5.973	2.977E-19	5.973
1280	4.709E-21	6.000	4.739E-21	6.000	4.665E-21	5.987	4.695E-21	5.987

Tab. 4.8: The eighth order scheme with $\beta = 1.92$, $\alpha = 0.59$, $k_d = 2$, $t_{end} = 1.0$ and CFL condition (4.28) for the heat equation with Dirichlet boundary conditions.

N	$C_a = 10^{-8}$, $C_b = 10^{-8}$				$C_a = 1 - 10^{-8}$, $C_b = 1 - 10^{-8}$			
	L^2 *error*	order	L^∞ *error*	order	L^2 *error*	order	L^∞ *error*	order
20	1.373E-11	–	1.745E-11	–	1.606E-11	–	1.897E-11	–
40	5.099E-14	8.073	7.182E-14	7.925	8.494E-14	7.562	1.105E-13	7.424
80	1.942E-16	8.036	2.851E-16	7.977	3.854E-16	7.784	5.255E-16	7.716
160	7.499E-19	8.017	1.120E-18	7.992	1.622E-18	7.893	2.263E-18	7.859
320	2.913E-21	8.008	4.386E-21	7.997	6.575E-21	7.946	9.278E-21	7.930

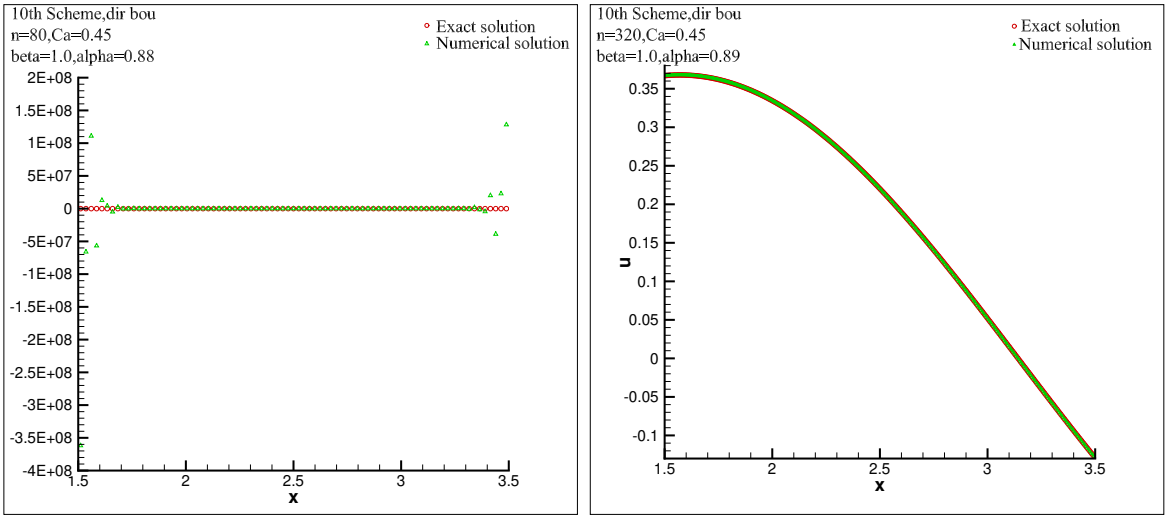

Fig. 4.22: The tenth order scheme and the new SILW method with $\beta = 1.0$, $k_d = 2$, $C_a = C_b = 0.45$, $t_{end} = 1.0$ and CFL condition (4.27). Left: $\alpha = 0.88$ and $N = 80$; Right: $\alpha = 0.89$ and $N = 320$.

- **The second order scheme**

At first, we explore $\beta = 0.5$ and $(k_d)_{min} = 1$. Take $\alpha \in [0.65, 1.90]$, then we can get a

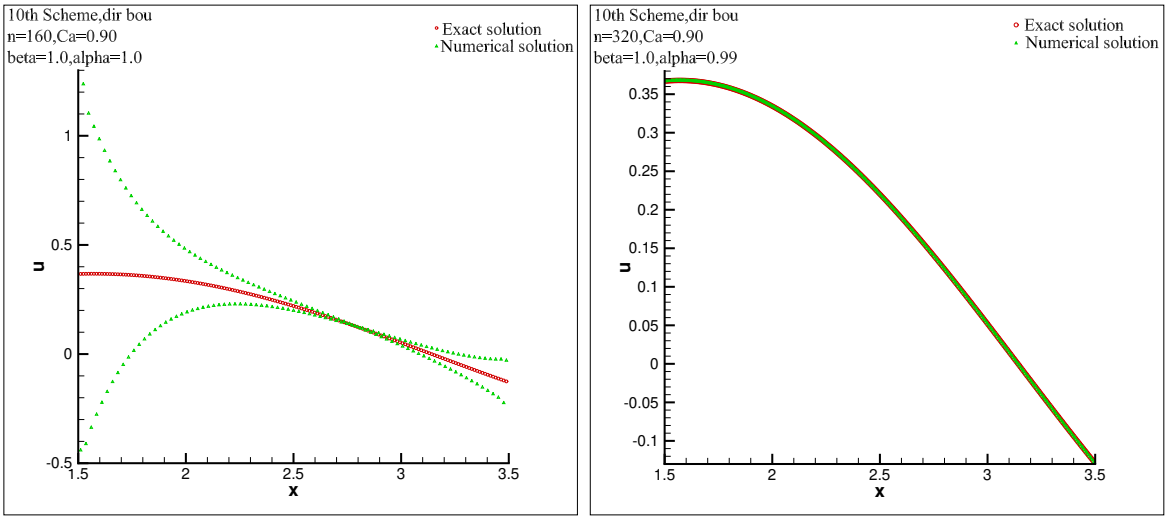

Fig. 4.23: The tenth order scheme and the new SILW method with $\beta = 1.0$, $k_d = 2$, $C_a = C_b = 0.90$, $t_{end} = 1.0$ and CFL condition (4.27). Left: $\alpha = 1.0$ and $N = 160$; Right: $\alpha = 0.99$ and $N = 320$.

Tab. 4.9: The tenth order scheme with $\beta = 0.46$, $\alpha = 1.69$, $k_d = 2$, $t_{end} = 1.0$ and CFL condition (4.27) for the heat equation with Dirichlet boundary conditions.

N	$C_a = 10^{-8}$, $C_b = 10^{-8}$				$C_a = 1 - 10^{-8}$, $C_b = 1 - 10^{-8}$			
	L^2 *error*	order	L^∞ *error*	order	L^2 *error*	order	L^∞ *error*	order
40	4.394E-12	–	4.419E-12	–	3.271E-12	–	3.290E-12	–
80	6.850E-14	6.003	6.893E-14	6.003	5.905E-14	5.792	5.942E-14	5.791
160	1.070E-15	6.001	1.077E-15	6.000	9.930E-16	5.894	9.992E-16	5.894
320	1.672E-17	6.000	1.682E-17	6.000	1.610E-17	5.946	1.620E-17	5.946
640	2.612E-19	6.000	2.628E-19	6.000	2.563E-19	5.973	2.579E-19	5.973
1280	4.081E-21	6.000	4.107E-21	6.000	4.043E-21	5.987	4.068E-21	5.987

stable scheme for all $C_a \in [0, 1)$, $C_b \in [0, 1)$. The left figures in Fig. 4.24 and Fig. 4.25 clearly show instability while the right ones show stability. A grid refinement verifies the designed second order with suitable α and β, see Tab. 4.11.

- **The fourth order scheme**

Take $\beta = 0.5$ and $(k_d)_{min} = 1$. To get a stable scheme for all $C_a \in [0, 1)$, $C_b \in [0, 1)$, the suitable choice of α is $\alpha \in [0.99, 1.33]$. Fig. 4.26 and 4.27 show the stability and instability results which is consistent with the analysis. Tab. 4.12 demonstrates that we can get the fourth order with small and large C_a and C_b for proper α and β.

- **The sixth order scheme**

Tab. 4.10: The tenth order scheme with $\beta = 0.46$, $\alpha = 1.69$, $k_d = 2$, $t_{end} = 1.0$ and CFL condition (4.29) for the heat equation with Dirichlet boundary conditions.

N	$C_a = 10^{-8}$, $C_b = 10^{-8}$				$C_a = 1 - 10^{-8}$, $C_b = 1 - 10^{-8}$			
	L^2 *error*	order	L^∞ *error*	order	L^2 *error*	order	L^∞ *error*	order
10	4.043E-10	–	3.633E-10	–	1.663E-10	–	1.478E-10	–
20	3.681E-13	10.101	4.324E-13	9.715	3.649E-13	8.832	4.124E-13	8.485
40	3.386E-16	10.086	4.428E-16	9.931	5.332E-16	9.419	6.741E-16	9.257
80	3.200E-19	10.047	4.377E-19	9.982	6.379E-19	9.707	8.482E-19	9.634
160	3.072E-22	10.023	4.289E-22	9.995	6.902E-22	9.852	9.389E-22	9.819

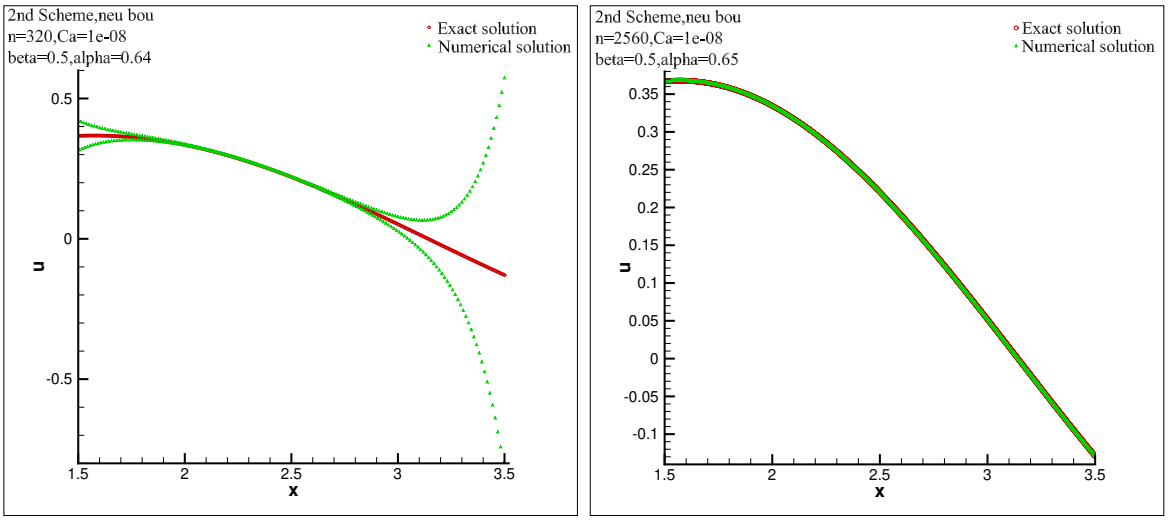

Fig. 4.24: The second order scheme and the new SILW method with $\beta = 0.5$, $k_d = 1$, $C_a = C_b = 10^{-8}$, $t_{end} = 1.0$ and CFL condition (4.27). Left: $\alpha = 0.64$ and $N = 320$; Right: $\alpha = 0.65$ and $N = 2560$.

Take $\beta = 0.3$ and $(k_d)_{min} = 1$. In this circumstance, We can take $\alpha \in [1.19, 1.46]$ to get a stable scheme for all $C_a \in [0, 1)$, $C_b \in [0, 1)$. The numerical results are shown in Fig. 4.28 and 4.29, which are consistent with the stability analysis. The results in Tab. 4.13 shows that the scheme is stable and can reach the designed with suitable α and β.

- **The eighth order scheme**

Take $\beta = 0.5$ and in this case, $(k_d)_{min} = 2$ and $\alpha \in [2.14, 2.15]$. Stability and instability results are presented in Fig. 4.30 and 4.31, which are consistent with stability analysis. The numerical results at the final time $t_{end} = 1.0$ are shown in Tab. 4.14. We can observe that our scheme is stable and high order accuracy for small and large C_a and C_b with suitable choice of α and β. Moreover, if take the CFL condition as (4.28), we can get the eighth order as Tab. 4.15.

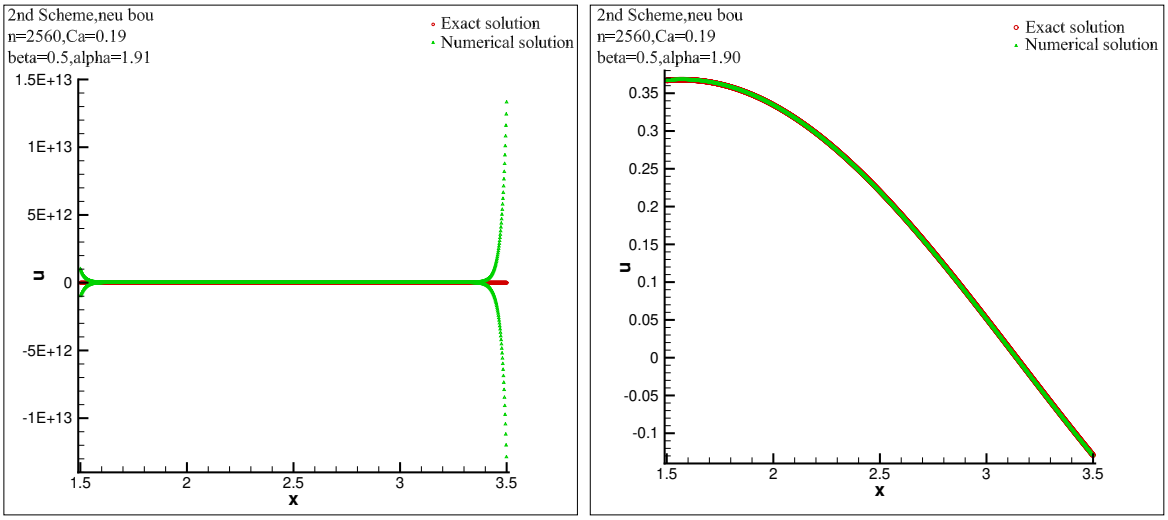

Fig. 4.25: The second order scheme and the new SILW method with $\beta = 0.5$, $k_d = 1$, $C_a = C_b = 0.19$, $t_{end} = 1.0$ and CFL condition (4.27). Left: $\alpha = 1.91$ and $N = 2560$; Right: $\alpha = 1.90$ and $N = 2560$.

Tab. 4.11: The second order scheme with $\beta = 5.0$, $\alpha = 0.18$, $k_d = 1$, $t_{end} = 1.0$ and CFL condition (4.27) for the heat equation with Neumann boundary conditions.

N	$C_a = 10^{-8}$, $C_b = 10^{-8}$				$C_a = 1 - 10^{-8}$, $C_b = 1 - 10^{-8}$			
	L^2 *error*	order	L^∞ *error*	order	L^2 *error*	order	L^∞ *error*	order
40	1.387E-04	–	2.028E-04	–	1.515E-04	–	2.256E-04	–
80	3.421E-05	2.020	5.071E-05	2.000	4.070E-05	1.896	6.009E-05	1.909
160	8.493E-06	2.010	1.268E-05	2.000	1.056E-05	1.947	1.548E-05	1.956
320	2.116E-06	2.005	3.169E-06	2.000	2.690E-06	1.973	3.931E-06	1.978
640	5.280E-07	2.003	7.923E-07	2.000	6.789E-07	1.986	9.900E-07	1.989
1280	1.319E-07	2.001	1.981E-07	2.000	1.705E-07	1.993	2.484E-07	1.995

- **The tenth order scheme**

Take $\beta = 1.36$ and $(k_d)_{min} = 4$. Here, we can take $\alpha \in [1.46, 1.66]$ to get a stable scheme for all $C_a \in [0, 1)$, $C_b \in [0, 1)$. Fig. 4.32 and 4.33 give the stable and unstable results. Tab. 4.16 shows that we can get the sixth order with small and large C_a and C_b for suitable α and β. If we take the CFL condition as (4.29), Tab. 4.17 indicates the optimal tenth order.

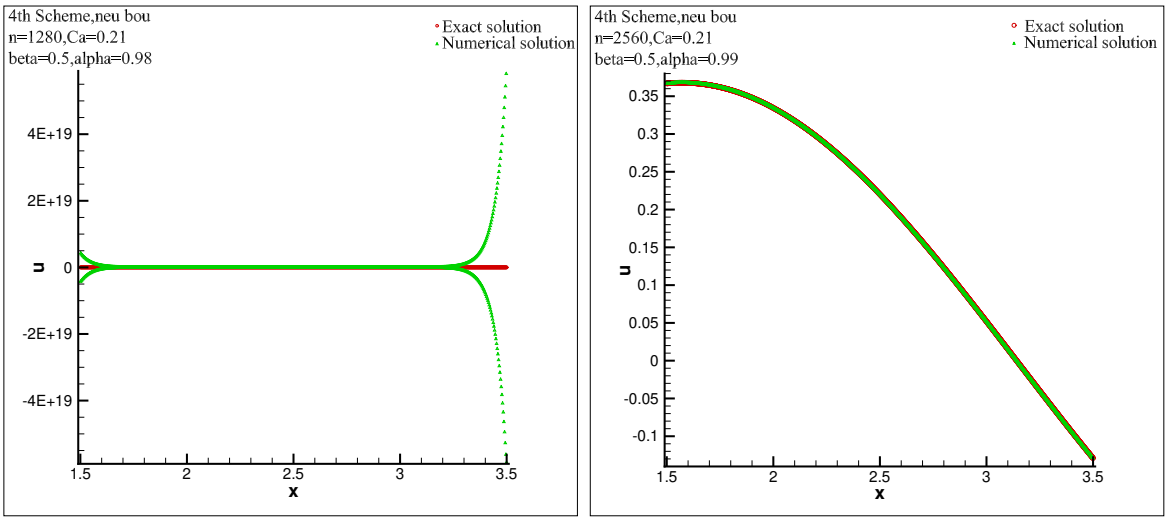

Fig. 4.26: The fourth order scheme and the new SILW method with $\beta = 0.5$, $k_d = 1$, $C_a = C_b = 0.21$, $t_{end} = 1.0$ and CFL condition (4.27). Left: $\alpha = 0.98$ and $N = 1280$; Right: $\alpha = 0.99$ and $N = 2560$.

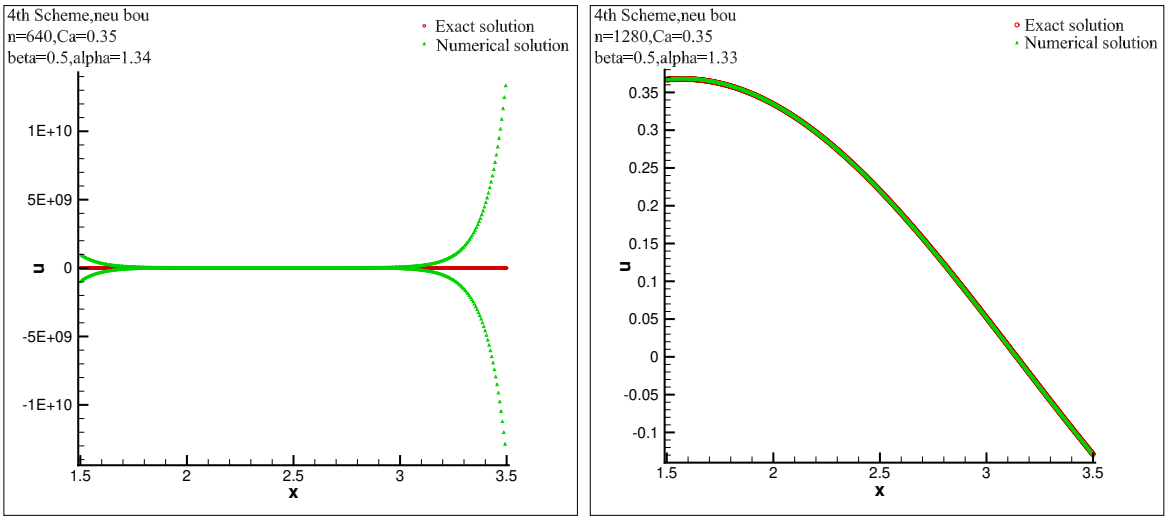

Fig. 4.27: The fourth order scheme and the new SILW method with $\beta = 0.5$, $k_d = 1$, $C_a = C_b = 0.35$, $t_{end} = 1.0$ and CFL condition (4.27). Left: $\alpha = 1.34$ and $N = 640$; Right: $\alpha = 1.33$ and $N = 1280$.

Tab. 4.12: The fourth order scheme with $\beta = 0.28$, $\alpha = 1.64$, $k_d = 1$, $t_{end} = 1.0$ and CFL condition (4.27) for the heat equation with Neumann boundary conditions.

N	$C_a = 10^{-8}$, $C_b = 10^{-8}$				$C_a = 1 - 10^{-8}$, $C_b = 1 - 10^{-8}$			
	L^2 *error*	order	L^∞ *error*	order	L^2 *error*	order	L^∞ *error*	order
40	4.021E-07	–	4.772E-07	–	2.651E-06	–	3.364E-06	–
80	2.529E-08	3.991	2.972E-08	4.005	1.899E-07	3.803	2.350E-07	3.840
160	1.586E-09	3.996	1.853E-09	4.004	1.271E-08	3.901	1.551E-08	3.921
320	9.923E-11	3.998	1.156E-10	4.002	8.223E-10	3.950	9.963E-10	3.961
640	6.206E-12	3.999	7.222E-12	4.001	5.229E-11	3.975	6.311E-11	3.981
1280	3.880E-13	4.000	4.512E-13	4.001	3.296E-12	3.988	3.971E-12	3.990

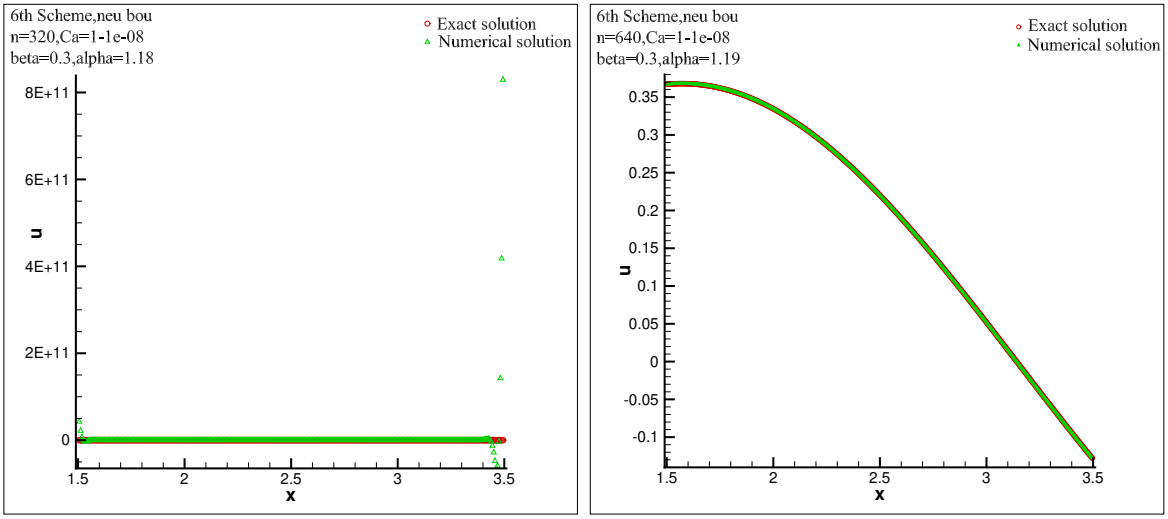

Fig. 4.28: The sixth order scheme and the new SILW method with $\beta = 0.3$, $k_d = 1$, $C_a = C_b = 1 - 10^{-8}$, $t_{end} = 1.0$ and CFL condition (4.27). Left: $\alpha = 1.18$ and $N = 320$; Right: $\alpha = 1.19$ and $N = 640$.

Tab. 4.13: The sixth order scheme with $\beta = 0.07$, $\alpha = 3.68$, $k_d = 1$, $t_{end} = 1.0$ and CFL condition (4.27) for the heat equation with Neumann boundary conditions.

N	$C_a = 10^{-8}$, $C_b = 10^{-8}$				$C_a = 1 - 10^{-8}$, $C_b = 1 - 10^{-8}$			
	L^2 *error*	order	L^∞ *error*	order	L^2 *error*	order	L^∞ *error*	order
40	1.457E-09	–	1.815E-09	–	1.627E-08	–	2.106E-08	–
80	2.316E-11	5.975	2.839E-11	5.998	3.090E-10	5.719	3.872E-10	5.766
160	3.646E-13	5.989	4.432E-13	6.001	5.322E-12	5.859	6.551E-12	5.885
320	5.718E-15	5.995	6.919E-15	6.001	8.731E-14	5.930	1.065E-13	5.943
640	8.950E-17	5.997	1.081E-16	6.001	1.398E-15	5.965	1.696E-15	5.972
1280	1.400E-18	5.999	1.688E-18	6.000	2.211E-17	5.982	2.676E-17	5.986

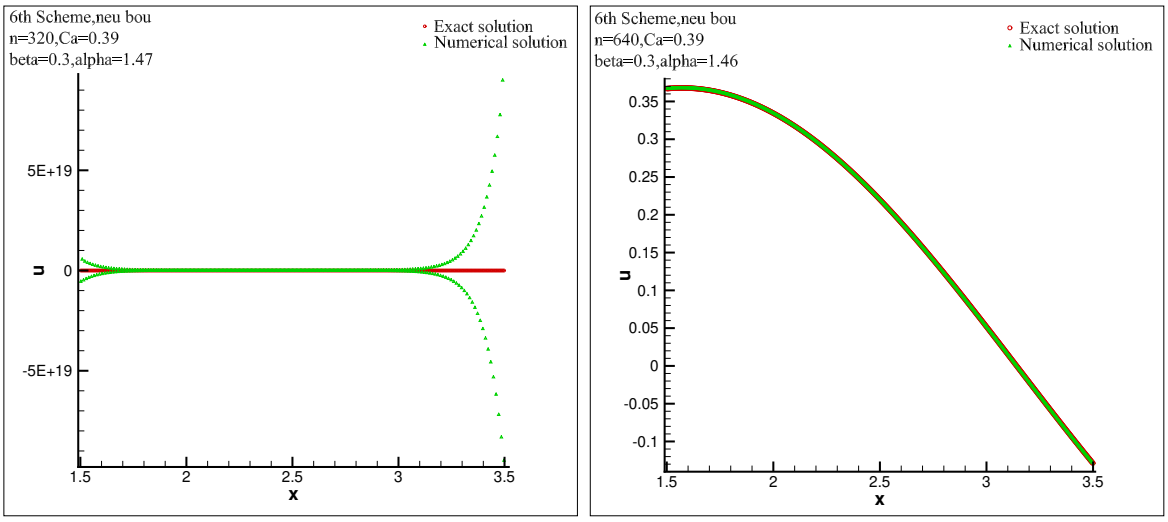

Fig. 4.29: The sixth order scheme and the new SILW method with $\beta = 0.3$, $k_d = 1$, $C_a = C_b = 0.39$, $t_{end} = 1.0$ and CFL condition (4.27). Left: $\alpha = 1.47$ and $N = 320$; Right: $\alpha = 1.46$ and $N = 640$.

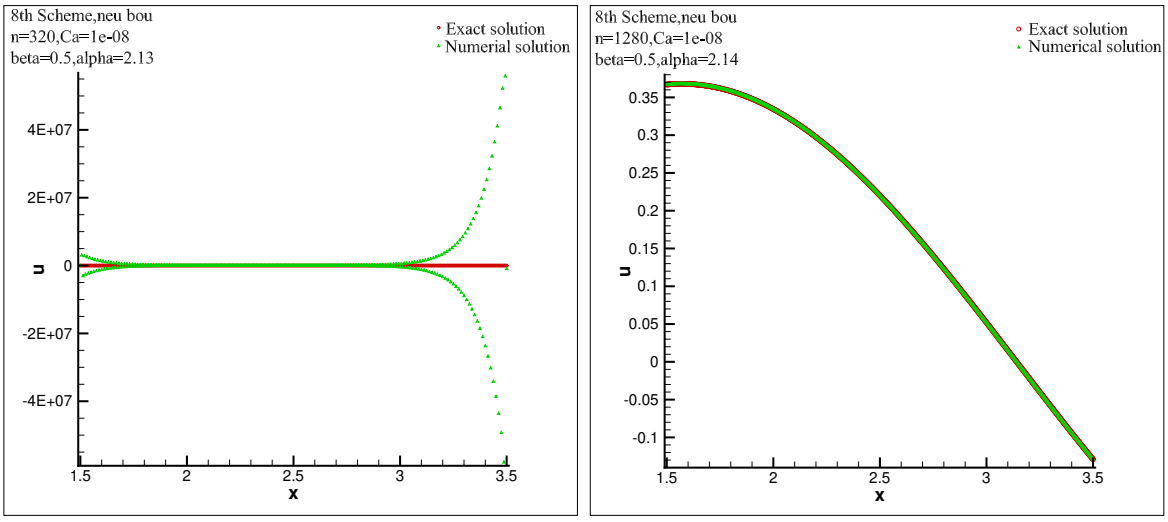

Fig. 4.30: The eighth order scheme and the new SILW method with $\beta = 0.5$, $k_d = 2$, $C_a = C_b = 10^{-8}$, $t_{end} = 1.0$ and CFL condition (4.27). Left: $\alpha = 2.13$ and $N = 320$; Right: $\alpha = 2.14$ and $N = 1280$.

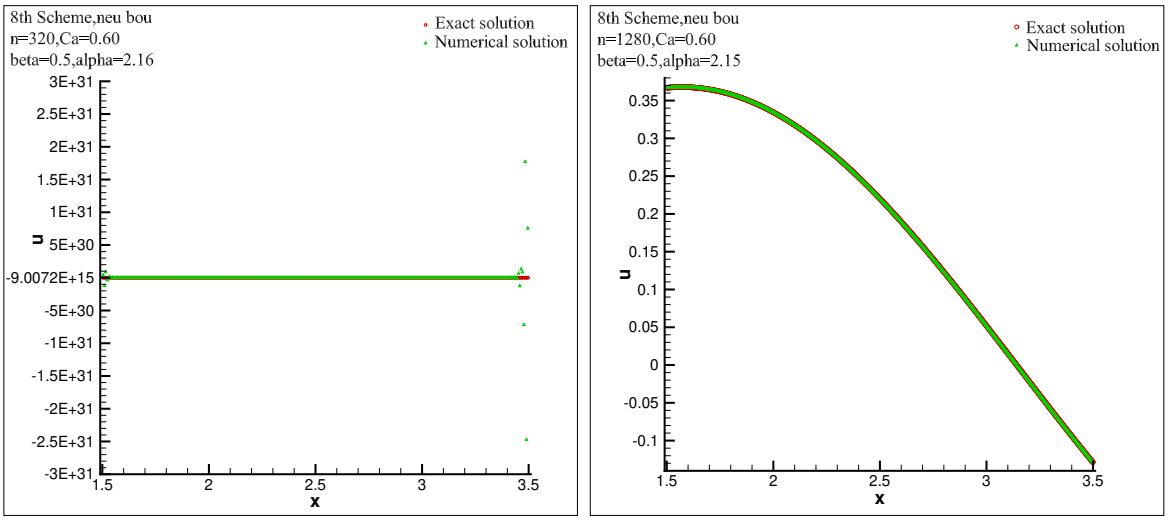

Fig. 4.31: The eighth order scheme and the new SILW method with $\beta = 0.5$, $k_d = 2$, $C_a = C_b = 0.60$, $t_{end} = 1.0$ and CFL condition (4.27). Left: $\alpha = 2.16$ and $N = 320$; Right: $\alpha = 2.15$ and $N = 1280$.

Tab. 4.14: The eighth order scheme with $\beta = 0.65$, $\alpha = 1.77$, $k_d = 2$, $t_{end} = 1.0$ and CFL condition (4.27) for the heat equation with Neumann boundary conditions.

N	$C_a = 10^{-8}$, $C_b = 10^{-8}$				$C_a = 1 - 10^{-8}$, $C_b = 1 - 10^{-8}$			
	L^2 *error*	order	L^∞ *error*	order	L^2 *error*	order	L^∞ *error*	order
40	1.754E-11	–	1.601E-11	–	9.962E-12	–	1.109E-11	–
80	2.731E-13	6.005	2.503E-13	5.999	2.156E-13	5.530	2.093E-13	5.728
160	4.258E-15	6.004	3.911E-15	6.000	3.848E-15	5.808	3.597E-15	5.863
320	6.643E-17	6.002	6.112E-17	6.000	6.346E-17	5.922	5.873E-17	5.937
640	1.037E-18	6.001	9.551E-19	6.000	1.015E-18	5.966	9.367E-19	5.970
1280	1.620E-20	6.001	1.492E-20	6.000	1.603E-20	5.984	1.478E-20	5.986

Tab. 4.15: The eighth order scheme with $\beta = 0.65$, $\alpha = 1.77$, $k_d = 2$, $t_{end} = 1.0$ and CFL condition (4.28) for the heat equation with Neumann boundary conditions.

N	$C_a = 10^{-8}$, $C_b = 10^{-8}$				$C_a = 1 - 10^{-8}$, $C_b = 1 - 10^{-8}$			
	L^2 *error*	order	L^∞ *error*	order	L^2 *error*	order	L^∞ *error*	order
10	5.293E-09	–	5.573E-09	–	7.144E-08	–	1.014E-07	–
20	1.737E-11	8.251	2.306E-11	7.917	7.102E-10	6.652	9.765E-10	6.699
40	6.627E-14	8.034	9.586E-14	7.910	4.520E-12	7.296	5.894E-12	7.372
80	2.588E-16	8.000	3.792E-16	7.982	2.259E-14	7.645	2.846E-14	7.694
160	1.013E-18	7.998	1.484E-18	7.997	9.983E-17	7.822	1.234E-16	7.850
320	3.960E-21	7.998	5.795E-21	8.000	4.148E-19	7.911	5.075E-19	7.926

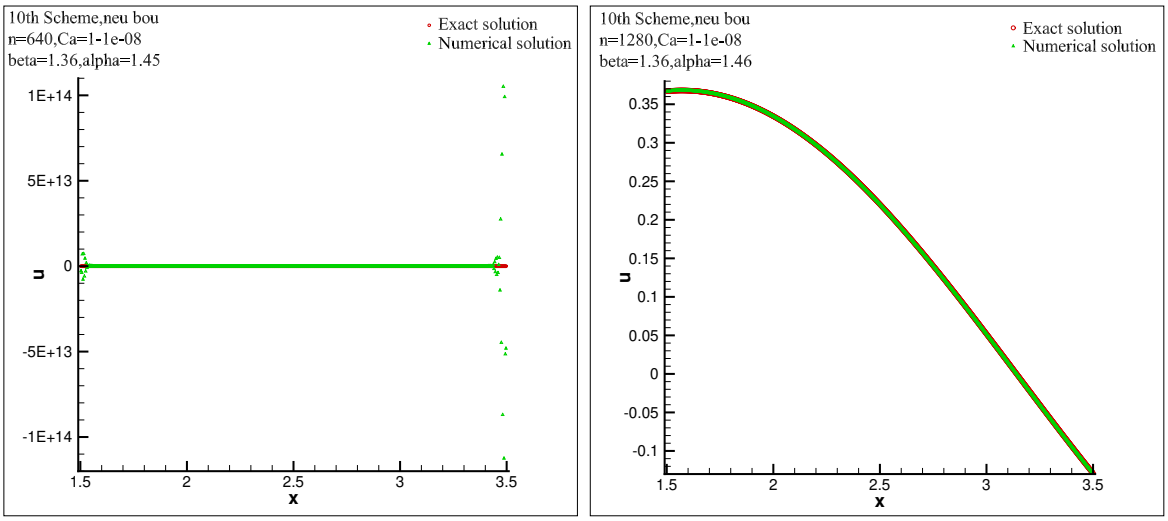

Fig. 4.32: The tenth order scheme and the new SILW method with $\beta = 1.36$, $k_d = 4$, $C_a = C_b = 1 - 10^{-8}$, $t_{end} = 1.0$. The CFL condition is in (4.27). Left: $\alpha = 1.45$ and $N = 640$; Right: $\alpha = 1.46$ and $N = 1280$.

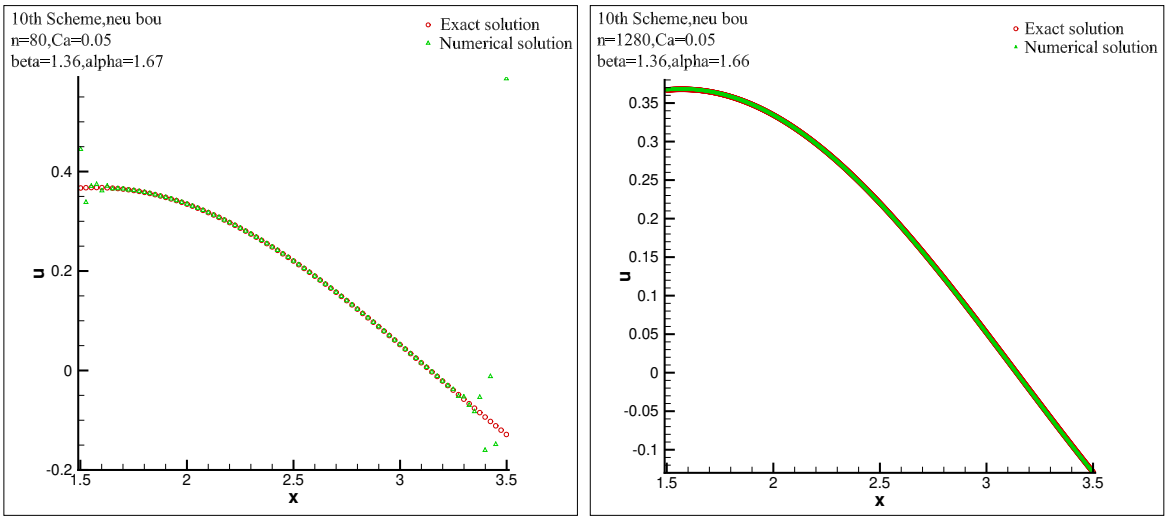

Fig. 4.33: The tenth order scheme and the new SILW method with $\beta = 1.36$, $k_d = 4$, $C_a = C_b = 0.05$, $t_{end} = 1.0$ and CFL condition (4.27). Left: $\alpha = 1.67$ and $N = 80$; Right: $\alpha = 1.66$ and $N = 1280$.

Tab. 4.16: The tenth order scheme with $\beta = 1.94$, $\alpha = 1.42$, $k_d = 4$, $t_{end} = 1.0$ and CFL condition (4.27) for the heat equation with Neumann boundary conditions.

N	$C_a = 10^{-8},\ C_b = 10^{-8}$				$C_a = 1 - 10^{-8},\ C_b = 1 - 10^{-8}$			
	L^2 *error*	order	L^∞ *error*	order	L^2 *error*	order	L^∞ *error*	order
40	1.527E-11	–	1.389E-11	–	1.113E-11	–	1.037E-11	–
80	2.370E-13	6.010	2.170E-13	6.001	2.018E-13	5.785	1.871E-13	5.792
160	3.690E-15	6.005	3.390E-15	6.000	3.404E-15	5.890	3.146E-15	5.894
320	5.757E-17	6.002	5.297E-17	6.000	5.528E-17	5.944	5.102E-17	5.946
640	8.988E-19	6.001	8.276E-19	6.000	8.807E-19	5.972	8.122E-19	5.973
1280	1.404E-20	6.001	1.293E-20	6.000	1.390E-20	5.986	1.281E-20	5.986

Tab. 4.17: The tenth order scheme with $\beta = 1.94$, $\alpha = 1.42$, $k_d = 4$, $t_{end} = 1.0$ and CFL condition (4.29) for the heat equation with Neumann boundary conditions.

N	$C_a = 10^{-8},\ C_b = 10^{-8}$				$C_a = 1 - 10^{-8},\ C_b = 1 - 10^{-8}$			
	L^2 *error*	order	L^∞ *error*	order	L^2 *error*	order	L^∞ *error*	order
10	9.045E-09	–	1.161E-08	–	3.609E-09	–	5.117E-09	–
20	1.026E-11	9.784	1.361E-11	9.737	1.061E-11	8.410	1.441E-11	8.472
40	1.077E-14	9.896	1.374E-14	9.952	1.840E-14	9.172	2.377E-14	9.244
80	1.085E-17	9.956	1.347E-17	9.995	2.405E-17	9.580	3.009E-17	9.626
160	1.074E-20	9.980	1.313E-20	10.002	2.719E-20	9.789	3.342E-20	9.814

5 Concluding Remarks

In this paper, we study the construction of numerical boundary conditions and stability analysis issue for high order central difference schemes for parabolic equation with both Dirichlet and Neumann boundary conditions on a finite domain. The new type of SILW method utilizes "interpolation" and "extrapolation" to get the values of the ghost points. First of all, we use the interior points to get a interpolation polynomial $p(x)$ and evaluate some artificial auxiliary point values by $p(x)$. Next, employ the values of artificial auxiliary points and spatial derivatives at boundary point obtained via the ILW procedure to get the extrapolation polynomial $q(x)$. Finally, approximation values of ghost points are got via $q(x)$. Appropriate selection of the artificial auxiliary points used in the new type of SILW method provides a powerful guarantee for the stability of the high order schemes for the diffusion equation with initial-boundary value conditions. Stability analysis is performed by both the Godunov-Ryabenkii analysis and the eigenvalue spectrum visualization method for semi-discrete and fully-discrete schemes. Although the eigenvalue spectrum visualization method is not as accurate as the Godunov-Ryabenkii analysis, but they can attain consistent results. Through stability analysis, we can get the range of β and $(k_d)_{min}$ where there exists a corresponding range of α to get a stable scheme for all $C_a \in [0, 1)$ and $C_b \in [0, 1)$ under the standard CFL condition for the corresponding periodic problems in Tab. 3.1. Numerical results not only validate the stability and instability results predicted by the analysis but also show the high order accuracy and efficiency of our schemes.

A Parameter selections for different schemes

Here, we present stability results of some different values of β and $(k_d)_{min}$ for both Dirichlet and Neumann boundary conditions for fully-discrete schemes in Sect. 2.1. Ranges of α which can ensure stability for all $C_a \in [0, 1)$ and $C_b \in [0, 1)$ under the standard CFL condition in Tab. 3.1 can be found in Tab. A.18–A.22.

Tab. A.18: range of α for different β for the 2nd scheme.

Dirichlet boundary condition with $k_d = 1$		Neumann boundary condition with $k_d = 1$	
β	α	β	α
0.1	[0.10,5.0]	0.01	[0.98,5.0]
0.64	[0.10,5.0]	0.56	[0.62,1.71]
1.19	[0.39,5.0]	1.12	[0.45,0.89]
1.73	[0.38,5.0]	1.67	[0.36,0.61]
2.28	[0.46,5.0]	2.23	[0.29,0.46]
2.82	[0.46,5.0]	2.78	[0.25,0.38]
3.37	[0.46,5.0]	3.34	[0.21,0.32]
3.91	[0.46,5.0]	3.89	[0.19,0.27]
4.46	[0.46,5.0]	4.45	[0.17,0.24]
5.0	[0.46,5.0]	5.0	[0.15,0.21]

Tab. A.19: range of α for different β for the 4th scheme.

Dirichlet boundary condition with $k_d = 1$		Neumann boundary condition with $k_d = 1$	
β	α	β	α
0.1	[4.88,5.0]	0.02	[4.27,5.0]
0.64	[1.03,3.4]	0.08	[1.75,5.0]
1.19	[0.65,2.19]	0.15	[1.24,3.72]
1.73	[0.49,1.66]	0.21	[1.12,2.80]
2.28	[0.40,1.34]	0.28	[1.07,2.20]
2.82	[0.33,1.13]	0.34	[1.04,1.87]
3.37	[0.29,0.98]	0.41	[1.01,1.59]
3.91	[0.26,0.86]	0.47	[0.99,1.41]
4.46	[0.23,0.77]	0.54	[0.98,1.23]
5.0	[0.21,0.70]	0.60	[1.0,1.08]

Tab. A.20: range of α for different β for the 6th scheme.

Dirichlet boundary condition with $k_d = 1$		Neumann boundary condition with $k_d = 1$	
β	α	β	α
0.39	[1.61,1.71]	0.03	[4.73,5.0]
0.90	[0.95,1.24]	0.07	[2.68,4.68]
1.41	[0.73,0.95]	0.11	[2.04,3.21]
1.93	[0.60,0.78]	0.15	[1.72,2.50]
2.44	[0.51,0.67]	0.19	[1.51,2.08]
2.95	[0.45,0.59]	0.24	[1.33,1.74]
3.46	[0.40,0.52]	0.28	[1.23,1.54]
3.98	[0.36,0.47]	0.32	[1.15,1.38]
4.49	[0.33,0.43]	0.36	[1.08,1.25]
5.0	[0.31,0.40]	0.40	[1.07,1.1]

Tab. A.21: range of α for different β for the 8th scheme.

Dirichlet boundary condition with $k_d = 2$		Neumann boundary condition with $k_d = 2$	
β	α	β	α
0.38	[1.99,2.11]	0.48	[2.21,2.21]
0.89	[0.90,1.32]	0.50	[2.14,2.15]
1.41	[0.61,0.88]	0.53	[2.03,2.08]
1.92	[0.48,0.70]	0.55	[1.97,2.03]
2.43	[0.42,0.60]	0.58	[1.88,1.97]
2.95	[0.37,0.52]	0.60	[1.82,1.93]
3.46	[0.33,0.46]	0.63	[1.75,1.87]
3.97	[0.30,0.42]	0.65	[1.71,1.83]
4.49	[0.28,0.38]	0.68	[1.70,1.78]
5.0	[0.26,0.35]	0.70	[1.71,1.73]

Tab. A.22: range of α for different β for the 10th scheme.

Dirichlet boundary condition with $k_d = 2$		Neumann boundary condition with $k_d = 4$	
β	α	β	α
0.46	[1.67,1.71]	1.07	[1.77,1.78]
0.96	[0.91,1.02]	1.17	[1.65,1.75]
1.47	[0.72,0.78]	1.26	[1.55,1.71]
1.97	[0.61,0.65]	1.36	[1.46,1.66]
2.48	[0.53,0.56]	1.46	[1.44,1.61]
2.98	[0.47,0.50]	1.55	[1.44,1.57]
3.49	[0.43,0.45]	1.65	[1.43,1.53]
3.99	[0.39,0.42]	1.75	[1.42,1.49]
4.50	[0.36,0.38]	1.84	[1.42,1.46]
5.0	[0.33,0.36]	1.94	[1.42,1.42]

References

[1] X.W. Bao, J. Yan and W.X. Sun, *A three dimensional tidal model in boundary-fitted curvilinear grids*, Coastal and Shelf Science, 50: 775–788, 2000.

[2] M.J. Berger, C. Helzel and R.J. Leveque, *H-box methods for the approximation of hyperbolic conservation laws on irregular grids*, SIAM J. Numer. Anal. 41: 893–918, 2003.

[3] M.H. Carpenter, D. Gottlieb, S. Abarbanel and W.-S. Don, *The theoretical accuracy of Runge-Kutta time discretizations for the initial boundary value problem: a study of the boundary error*, SIAM J. Sci. Comput. 16: 1241–1252, 1995.

[4] S. Ding, C.-W. Shu and M. Zhang, *On the conservation of finite difference WENO schemes in non-rectangular domains using the inverse Lax-Wendroff boundary treatments*, J. Comput. Phys. 415, 2020.

[5] S.K. Godunov and V.S. Ryabenkii, *Spectral stability criteria for boundary-value problems for non-self-adjoint difference equations*, (Russian) Uspehi Mat. Nauk 18: 3–14, 1963.

[6] B. Gustafsson, H.-O. Kreiss and J. Oliger, *Time-dependent problems and difference methods*, Wiley-Interscience, 1972.

[7] B. Gustafsson, H.-O. Kreiss and A. Sundström, *Stability theory of difference approximations for mixed initial boundary value problem. II*, Math. Comp. 26: 649–686, 1972.

[8] Y. Jiang, C.-W. Shu and M. Zhang, *Free-stream preserving finite difference schemes on curvilinear meshes*, Methods Appl. Anal. 21: 1–30, 2014.

[9] H.-O. Kreiss, *Stability theory for difference approximations of mixed initial boundary value problems. I*, Math. Comp. 27: 703–714, 1968.

[10] H.-O. Kreiss and N.A. Petersson, *A second order accurate embedded boundary method for the wave equation with Dirichlet data*, SIAM J. Sci. Comput. 27: 1141–1167, 2006.

[11] T. Li, J. Lu and C.-W. Shu, *Stability analysis of inverse Lax-Wendroff boundary treatment of high order compact difference schemes for parabolic equations*, J. Comput. Appl. Math. 400: 113711, 2022.

[12] T. Li, J. Lu and P. Wang, *Stability analysis of inverse Lax-Wendroff procedure for a high order compact finite difference schemes*, Commun. Appl. Math. Comput. 6: 142-189, 2024.

[13] T. Li, C.-W. Shu and M. Zhang, *Stability analysis of the inverse Lax-Wendroff boundary treatment for high order upwind-biased finite difference schemes*, J. Comput. Appl. Math. 299: 140–158, 2016.

[14] T. Li, C.-W. Shu and M. Zhang, *Stability Analysis of the Inverse Lax-Wendroff Boundary Treatment for High Order Central Difference Schemes for Diffusion Equations*, J. Sci. Comput. 70: 576–607, 2017.

[15] S. Liu, *Development and application of high order ILW method for complex boundary*, PhD thesis from University of Science and Technology of China (in Chinese), 2022.

[16] S. Liu, T. Li, Z. Cheng, Y. Jiang, C.-W. Shu and M. Zhang, *A new type of simplified inverse Lax-Wendroff boundary treatment I: hyperbolic conservation laws*, J. Comput. Phys. 514: 113259, 2024.

[17] J. Lu, J. Fang, S. Tan,C.-W. Shu and M. Zhang, *Inverse Lax-Wendroff procedure for numerical boundary conditions of convection-diffusion equations*, J. Comput. Phys. 317: 276–300, 2016.

[18] J. Lu, C.-W. Shu, S. Tan and M. Zhang, *An inverse Lax-Wendroff procedure for hyperbolic conservation laws with changing wind direction on the boundary*, J. Comput. Phys. 426, 2021.

[19] S. Osher, *Stability of difference approximations of dissipative type for mixed initial-boundary value problems*, Math. Comp. 23: 335–340, 1969.

[20] S. Osher, *Stability of parabolic difference approximations to certain mixed initial boundary value problems*, Math. Comp. 26: 13-39, 1972.

[21] K. Otto and M. Thuné, *Stability of a Runge-Kutta method for the Euler equations on a substructured domain*, SIAM J. Scien Stat. Comput. 10: 154–174, 1989.

[22] C.-W. Shu and S. Osher, *Efficient implementation of essentially non-oscillatory shock-capturing schemes*, J. Comput. Phys. 77: 439–471, 1988.

[23] B. Sjögreen and N.A. Petersson, *A Cartesian embedded boundary method for hyperbolic conservation laws*, Commun. Comput. Phys. 2: 1199–1219, 2007.

[24] D.M. Sloan, *Boundary conditions for a fourth order hyperbolic difference scheme*, Math. Comput. , 41: 1–11, 1983.

[25] E. Sousa, *A Godunov-Ryabenkii instability for a Quickest scheme*, Lecture Notes Comput. Sci. , 1988: 732–740, 2001.

[26] E. Sousa, *Stability analysis of difference methods for parabolic initial value problems*, J. Sci. Comput, 26: 45–66, 2006.

[27] J.C. Strikwerda, *Initial boundary value problems for the method of lines*, J. Comput. Phys. 34: 94-107, 1980.

[28] S. Tan and C.-W. Shu, *Inverse Lax-Wendroff procedure for numerical boundary conditions of conservation laws*, J. Comput. Phys. 229: 8144–8166, 2010.

[29] S. Tan and C.-W. Shu, *A high order moving boundary treatment for compressible inviscid flows*, J. Comput. Phys. 230: 6023–6036, 2011.

[30] S. Tan, C. Wang, C.-W. Shu and J. Ning, *Efficient implementation of high order inverse Lax-Wendroff boundary treatment for conservation laws*, J. Comput. Phys. 231: 2510–2527, 2012.

[31] J.M. Varah, *Stability of difference approximations to the mixed initial boundary value problems for parabolic systems*, SIAM J. Numer. Anal. 8: 598–615, 1971.

[32] F. Vilar and C.-W. Shu, *Development and stability analysis of the inverse Lax-Wendroff boundary treatment for central compact schemes*, ESAIM Math. Model. Numer. Anal. 49: 39–67, 2015.